

# Preliminary ranking of alternative scalar and vector intensity measures of ground shaking

Hossein Ebrahimian<sup>1</sup> · Fatemeh Jalayer<sup>1</sup> ·  
Andrea Lucchini<sup>2</sup> · Fabrizio Mollaioli<sup>2</sup> ·  
Gaetano Manfredi<sup>1</sup>

Received: 24 September 2014 / Accepted: 26 March 2015 / Published online: 12 April 2015  
© Springer Science+Business Media Dordrecht 2015

**Abstract** In Performance-Based Earthquake Engineering, seismic demand in structures is predicted by building probabilistic seismic demand models that link measures of earthquake intensity (*IMs*) to measures of structural demand. Investigations are carried out herein for evaluating the predictive capability of a wide range of commonly-used scalar and vector-valued *IMs* for different peak-related demand parameters. To accomplish this goal, both efficiency and sufficiency of the candidate *IMs* are taken into account. The latter is evaluated with the recently-proposed “*relative sufficiency measure*”. This measure, which is derived based on information theory concepts, quantifies the amount of information gained (on average) by an *IM* relative to another about the demand parameter of interest. Evaluation of the *IMs*, herein, uses two sets of ground motions consisting of

---

An early version of this work were presented in the Second European Conference on Earthquake Engineering and Seismology (2ECEES), Istanbul, Turkey, August 24–29.

---

**Electronic supplementary material** The online version of this article (doi:[10.1007/s10518-015-9755-9](https://doi.org/10.1007/s10518-015-9755-9)) contains supplementary material, which is available to authorized users.

---

✉ Hossein Ebrahimian  
ebrahimian.hossein@unina.it

Fatemeh Jalayer  
fatemeh.jalayer@unina.it

Andrea Lucchini  
andrea.lucchini@uniroma1.it

Fabrizio Mollaioli  
fabrizio.mollaioli@uniroma1.it

Gaetano Manfredi  
gamanfre@unina.it

<sup>1</sup> Department of Structures for Engineering and Architecture, University of Naples Federico II, Via Claudio 21, 80125 Naples, Italy

<sup>2</sup> Department of Structural and Geotechnical Engineering, University of Rome “La Sapienza”, Via Gramsci 53, 00197 Rome, Italy

ordinary and pulse-like near-fault records. Two-dimensional RC frame structures, both fixed and isolated at the base, are selected. The most suitable *IMs* for predicting the considered different demand parameters and types of structure are identified in terms of both efficiency and sufficiency. The use of these most informative *IMs* is suggested to build improved probabilistic demand models.

**Keywords** Performance-based seismic assessment · Intensity measure · Ground motion record selection · Information theory · Relative entropy · Relative Sufficiency · Base-isolated building

## 1 Introduction

In the context of Performance Based Earthquake Engineering (PBEE, Cornell and Krawinkler 2000; Moehle and Deierlein 2004), seismic risk for a structure can be expressed in terms of the mean annual frequency (MAF) of exceeding a specified limit state,  $\lambda_{LS}$ . In this methodology, uncertainty in the ground motion intensity is described with a scalar parameter, or a low-dimensional vector of parameters, called intensity measure (*IM*) (Shome et al. 1998; Jalayer and Cornell 2003; Luco and Cornell 2007; Jalayer and Cornell 2009). This is a simplified way to represent ground motion uncertainty, which is alternative to the rigorous approach consisting in a full probabilistic description of the ground-motion time history by means of a stochastic model (see e.g., Jalayer and Beck 2008). The *IM* serves as an intermediate variable between ground motion hazard and structural demand estimates, which are linked as follows:

$$\lambda_{LS} = \int_{im} P[D > C_{LS}|IM = im] |d\lambda_{IM}(im)| \quad (1)$$

where  $D$  denotes the structural demand (a.k.a. engineering demand parameter);  $C_{LS}$  is the capacity of the structure associated with the prescribed limit state  $LS$ ;  $\lambda_{IM}$  is the seismic hazard expressed in terms of MAF of exceeding a certain level of *IM* at the site; and finally  $P[D > C_{LS}|IM]$  is the conditional probability that demand  $D$  exceeds the limit state capacity  $C_{LS}$  which is known as the structure fragility.

It is clear that in PBEE, the selection of a suitable *IM* for representing ground motion uncertainty is a major concern that has to be addressed. The stronger is the correlation between the predicted  $D$  and the adopted *IM*, the more accurate will be the result of the probabilistic risk assessment. Currently, the properties that are considered for measuring the suitability of an *IM* in representing the dominant features of ground shaking are the sufficiency, the efficiency, the scaling robustness, and the predictability through a probabilistic seismic hazard analysis (see Shome and Cornell 1999; Giovenale et al. 2004; Luco and Cornell 2007). Among these properties, the first two are of particular concern within the present study. An *efficient IM* leads to a relatively small variability of  $D|IM$ ; consequently, a small number of ground motions and nonlinear dynamic analyses is required to estimate with adequate precision the conditional probability distribution  $P[D|IM]$ . A *sufficient IM*, on the other hand, is one that makes the probability distribution  $P[D|IM]$  independent of other ground motion characteristics; hence, using a sufficient *IM* implies that a detailed ground-motion record selection is not necessary while keeping the same accuracy in seismic structural performance estimation.

Efficiency and sufficiency of *IMs* have been the focus of attention of many researchers. For instance, Shome et al. (1998) demonstrated that the 5 %-damped pseudo-spectral acceleration at the first-mode period  $Sa(T_1)$  is more efficient than the peak ground acceleration *PGA*. Nonetheless, for tall and long-period buildings as well as for structures subjected to near-source ground motions,  $Sa(T_1)$  may not be neither efficient nor sufficient because of the limited spectral shape information (see Shome and Cornell 1999; Luco and Cornell 2007). This is in part due to the fact that  $Sa(T_1)$  accounts neither for contribution of higher modes nor for period lengthening owing to structural nonlinearity.

Several alternative *IMs* were proposed as multiplicative adjustments of  $Sa(T_1)$  in order to explicitly overcome the aforementioned drawbacks (Shome and Cornell 1999; Cordova et al. 2000; Mori et al. 2004; Luco and Cornell 2007; Bianchini et al. 2009; Lin et al. 2011). The objective of these proposals is not only to improve the predictive efficiency of the *IM* for all damage levels of a given structure, but also to account for the *IM* computability through a ground-motion hazard analysis without the need of any new attenuation relationships. Moreover, numerous spectrum-based scalar *IMs* including energy-derived ones were investigated, and studies showed that velocity-based *IMs* are in general better correlated to deformation demands especially in the case of medium rise frame structures (Akkar and Özen 2005; Riddell 2007; Yakut and Yilmaz 2008; Jayaram et al. 2010; Mollaioli et al. 2011). In Jayaram et al. (2010) and Mollaioli et al. (2011), the effect of near-fault ground motions and different soil types was also taken into account in evaluating predictive capabilities of the prescribed *IMs*.

As opposed to a scalar *IM*, a vector-valued one is a vector of more than one *IM*, which commonly comprises of two parameters. The vector-valued *IM* consisting of  $Sa(T_1)$  and spectral values at other periods was shown to be a good predictor for ordinary ground motions (Luco et al. 2005; Vamvatsikos and Cornell 2005; Baker and Cornell 2008a) as well as for pulse-like ground motions (Baker and Cornell 2008b). The vector-valued *IM* consisting of  $Sa(T_1)$  and  $\varepsilon$  (defined as the number of standard deviations by which  $\ln Sa(T_1)$  differs from its predicted mean value obtained from a ground motion prediction model) was thoroughly investigated by Baker and Cornell (2006). The above mentioned vector-valued *IMs* provide more information about the shape of a record's response spectrum.

This study aims at investigating the predictive capability of a wide range of scalar and vector-valued *IMs* by taking into account both ordinary and pulse-like near fault ground motions. In order to achieve this goal, efficiency and sufficiency of the considered *IMs* are assessed. Usually, logarithmic linear regression of the structural response parameter  $D$  conditioned on the considered scalar or vector-valued *IM* is carried out to define a probabilistic model for  $P[D|IM]$ . This probabilistic model is then used to evaluate efficiency and sufficiency of the prescribed *IM*. The standard error of regression  $\sigma_{\ln D|IM}$  is considered as a measure of the *IM* efficiency, while a linear regression analysis of the residuals of  $\ln D|IM$  relative to the ground motion parameters (e.g., magnitude  $M$ , distance  $R$ , and  $\varepsilon$ ) is usually carried out for evaluating the *IM* sufficiency. Accordingly, the significance of having a linear trend implies the amount of insufficiency associated with the desired *IM*, which is usually measured by the  $p$  value of the estimated slope (see Luco and Cornell 2007).

Nevertheless, establishing sufficiency in an absolute sense is likely to require high-dimensional vector *IMs* since it involves independence of  $D|IM$  from other ground motion characteristics for all possible values of the *IM*. Hence, for a scalar or a low-dimensional vector *IM*, it is more reasonable to examine sufficiency in a relative sense. In this case, the suitability of one *IM* with respect to another could be evaluated in terms of the average difference in information provided about the predicted  $D$ . By using the concept of relative

entropy from information theory, Jalayer et al. (2012) introduced a measure, called *relative sufficiency measure* (RSM). The RSM of  $IM_1$  with respect to  $IM_2$  quantifies on average how much more information  $IM_1$  relays to the designated structural response parameter  $D$  about the ground motion with respect to  $IM_2$ .

This study intends to apply the RSM to measure the suitability of alternative  $IM$ s in predicting various demand parameters, and to provide a preliminary ranking of them. To fulfil this objective, two RC buildings consisting of a 4-story and a 6-story moment-resisting frame are employed. The frames are two-dimensional structures in order to avoid further concerns related to the study of  $IM$ s that explicitly account for possible torsional behaviors (for more details, see Lucchini et al. 2011). The two structures are designed according to a past Italian code (DM 96; 1996) and can be representative of regular existing RC buildings located in high seismic zones of the Mediterranean area. Both cases of the case-study structures being fixed and isolated at the base are considered herein. These buildings have been recently used by Mollaioli et al. (2013) and Ebrahimian et al. (2014) for a systematic evaluation of a large set of scalar  $IM$ s with respect to the seismic demand prediction of buildings. It is important to underline that in Mollaioli et al. (2013), the  $IM$  sufficiency is simply evaluated by measuring the independence of the conditional probability distribution  $P[D|IM]$  from magnitude and distance only. However, in this work the RSM is used as a robust measure of sufficiency. The set of  $IM$ s used in this study comprises those investigated by Mollaioli et al. (2013) in addition to other multi-parameter scalar and vector-valued  $IM$ s, which account for the period lengthening and/or higher mode effect. It should be noted that the RSM is particularly suitable for measuring the relative sufficiency of vector-valued  $IM$ s (e.g., vector  $IM$ s of more than two components). This provides the capability of studying candidate vector-valued  $IM$ s that are most suitable for pulse-like ground motion records.

As a result, this work provides sets of suitable  $IM$ s based on both efficiency and sufficiency criteria for different type of base fixities as well as different type of ground motions (i.e., ordinary and pulse-like). The outcomes reveal perfect correlation between relative sufficiency and efficiency of suitable  $IM$ s. It is shown that the results of the quantitative-evaluations of the sufficiency obtained by using the RSM agree quite well with the conclusions of Mollaioli et al. (2013). Findings and conclusions drawn in following sections are mainly applicable to buildings similar to those investigated in the present study, that is, existing medium-rise RC frames typical of high-intensity seismic zones of the Mediterranean area.

## 2 Intensity measures and demand parameters

The set of scalar and vector-valued  $IM$ s as well as the demand parameters used herein are summarized as follows. It is noteworthy that this paper focuses on the set of elastic  $IM$ s and the inelastic energy-based  $IM$ s (see e.g. Nurtuğ and Sucuoğlu 1995; Sucuoğlu and Erberik 2004; Kalkan and Kunnath 2007) are not discussed herein.

### 2.1 Scalar $IM$ s

Figure 1 outlines the general categorization of scalar  $IM$ s used in this study, which are summarized in Table 1. The set of scalar  $IM$ s includes those used in the comparative study by Mollaioli et al. (2013) for predicting seismic demands in base-isolated structures, which

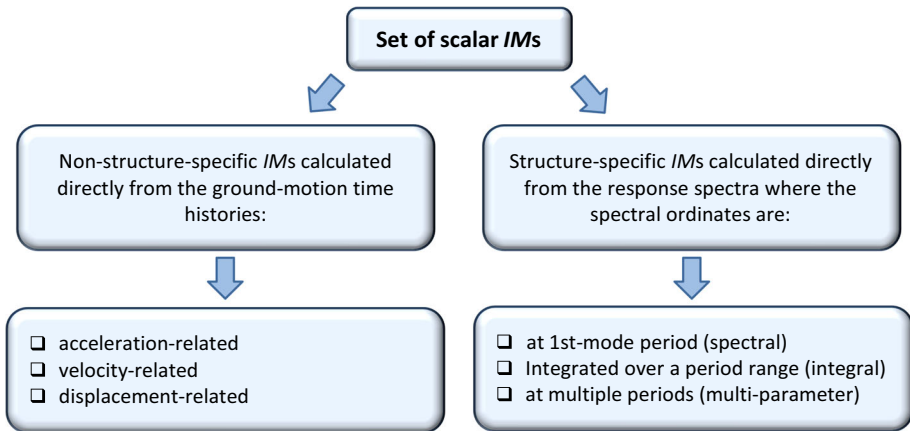


**Fig. 1** Categorization of the set of scalar *IMs*

are composed of two general subsets: (1) 14 non-structure-specific *IMs* comprising of acceleration-, velocity-, and displacement-related *IMs*; (2) 13 structure-specific *IMs* dividing into spectral and integral ones. All the spectral values are estimated at 5 % damping. In addition, 5 structure-specific multi-parameter scalar *IMs* that account for the period lengthening and/or higher-mode effect are considered in this work (see Fig. 1 for a brief outline).

The set of *IMs* proposed by Mollaioli et al. (2013) is composed of most commonly used ones in literature together with new integral *IMs*, which were obtained by modifying the existing ones in order to get better correlation with the predicted demands. Integral-based structure-specified *IMs* (see Table 1) are evaluated by integration of the spectral values over a given period range in order to explicitly account for higher-mode effects as well as period lengthening due to structural softening. In this group, the so-called “modified” *IMs* are obtained from the existing *IMs* by changing the period range of integration. For the fixed-base buildings, Mollaioli et al. (2013) suggested the integration interval to be  $[0.2T_1, 1.5T_1]$  where  $T_1$  is the first-mode period of the structure. Similarly, the interval was set to  $[0.5T_{ip}, 1.25T_{ip}]$  for base-isolated structures where  $T_{ip}$  is the isolation period. This period range was also suggested by Avsar and Özdenmir (2013). The aforementioned intervals are more-or-less used as a basis for defining the corresponding period-range in multi-parameter scalar *IMs*, which are defined as follows:

- (a) The *IM* proposed by Cordova et al. (2000) which is expressed as follows:

$$S^*(T_1, C, \alpha) = Sa(T_1) \left( \frac{Sa(CT_1)}{Sa(T_1)} \right)^\alpha \tag{2}$$

where  $CT_1$  ( $C > 1$ ) accounts for period elongation which reflects softening of an inelastic structure. Cordova et al. (2000) suggested values of  $C = 2$  and  $\alpha = 0.5$  by optimizing the efficiency of their proposed *IM* for a set of model structures and earthquake records. For the base-isolated structure herein,  $T_{ip}$  is used in place of  $T_1$ , and  $C = 1.25$ .

**Table 1** *IMs* considered in this study

Category	Class	Intensity Measure ( <i>IM</i> )		
		Notation	Definition/references	
Non-structure-specific scalar <i>IMs</i>	Acceleration-related (see Mollaioli et al. 2013)	<i>PGA</i>	Peak ground acceleration	
		<i>AI</i>	Arias intensity	
		<i>CAV</i>	Cumulative absolute velocity	
		<i>I<sub>a</sub></i>	Compound acceleration-related intensity	
		<i>I<sub>c</sub></i>	Characteristic intensity	
		Velocity-related (see Mollaioli et al. 2013)	<i>PGV</i>	Peak ground velocity
			<i>FI</i>	Fajfar intensity
	<i>I<sub>v</sub></i>		Compound velocity-related intensity	
	<i>CAD</i>		Cumulative absolute displacement	
	<i>IV</i>		Incremental velocity	
	Displacement-related (see Mollaioli et al. 2013)	<i>SED</i>	Specific energy density	
		<i>PGD</i>	Peak ground displacement	
		<i>I<sub>d</sub></i>	Compound displacement-related intensity	
		<i>ID</i>	Incremental displacement	
		Structure-specific scalar <i>IMs</i>	Spectral (see Mollaioli et al. 2013)	<i>Sa</i>
<i>E<sub>Ir</sub></i>	Relative input energy			
<i>E<sub>Ia</sub></i>	Absolute input energy			
Integral (see Mollaioli et al. 2013)	<i>ASI</i>		Acceleration spectrum intensity	
	<i>VSI</i>		Velocity spectrum intensity	
	<i>I<sub>H</sub></i>		Housner intensity	
	<i>V<sub>EIrSI</sub></i>		Relative input equivalent energy <i>VSI</i>	
	<i>V<sub>EIaSI</sub></i>		Absolute input equivalent energy <i>VSI</i>	
	<i>MASI</i>		Modified <i>ASI</i>	
	<i>MVSI</i>		Modified <i>VSI</i>	
	<i>MI<sub>H</sub></i>		Modified <i>I<sub>H</sub></i>	
	<i>MV<sub>EIrSI</sub></i>		Modified <i>V<sub>EIrSI</sub></i>	
	<i>MV<sub>EIaSI</sub></i>		Modified <i>V<sub>EIaSI</sub></i>	
	Multi-parameter		<i>S*</i>	Cordova et al. (2000)
			<i>Sa<sub>avg</sub>(<b>T</b>*)<sup>a</sup></i>	Bianchini et al. (2009)
<i>S<sub>N1</sub>, S<sub>N2</sub></i>		Lin et al. (2011)		
Vector-valued <i>IMs</i>		<i>[PGA, M]</i>	Elefante et al. (2010)	
		<i>[Sa(T<sub>1</sub>), R<sub>T<sub>1</sub>,T*</sub>]<sup>b</sup></i>	Baker and Cornell (2008a, b)	
		<i>[Sa(T<sub>1</sub>), ε]</i>	Baker and Cornell (2006)	
		<i>[Sa(T<sub>1</sub>), R<sub>T<sub>1</sub>,T*, ε]<sup>b</sup></sub></i>	Baker and Cornell (2008a)	

<sup>a</sup> Two different vectors for **T**\* are assigned to this scalar *IM* (see Sect. 2.1)

<sup>b</sup> Two different values for *T*\* are assigned to this vector-valued *IM* (see Sect. 2.2)

- (b) The *IM* proposed by Bianchini et al. (2009):

$$Sa_{avg}(\mathbf{T}^*) = Sa_{avg}(T^{(1)}, \dots, T^{(n)}) = \left( \prod_{i=1}^n Sa(T^{(i)}) \right)^{\frac{1}{n}} \tag{3}$$

where  $\mathbf{T}^* = [T^{(1)}, \dots, T^{(n)}]$  is the vector of  $n$  periods of interest, and  $Sa_{avg}$  is the geometric mean of  $Sa$  ordinates calculated at those periods. Bianchini et al. (2009) recommended that  $Sa_{avg}$  should be calculated at least at  $n = 10$  logarithmically-spaced points (this treatment is more efficient than considering the same number of periods being arithmetically spaced). Accordingly, two different period-intervals were proposed: (1)  $\mathbf{T}_1^* = [T_1, \dots, 2T_1]$  which was suggested for the first-mode dominant (low period structures), (2)  $\mathbf{T}_2^* = [0.2T_1, \dots, 2T_1]$  suggested for structures with medium-to-long periods affected by higher modes. Comparably, for the base-isolated structures herein, the period-intervals are consistently set to  $\mathbf{T}_1^* = [T_{ip}, \dots, 1.25T_{ip}]$  and  $\mathbf{T}_2^* = [0.5T_{ip}, \dots, 1.25T_{ip}]$ .

- (c) Two *IMs* proposed by Lin et al. (2011) are expressed as follows:

$$\begin{aligned} S_{N1} &= Sa(T_1)^\alpha \cdot Sa(CT_1)^{1-\alpha} \\ S_{N2} &= Sa(T_1)^\beta \cdot Sa(T_2)^{1-\beta} \end{aligned} \tag{4}$$

These two *IMs* take into account the issues related to period elongation (i.e.,  $S_{N1}$ ) and the second mode effects considering  $T_2$  as the 2nd-mode period (denoted as  $S_{N2}$ ), independently. By optimizing the efficiency, Lin et al. (2011) suggested  $C = 1.5$ ,  $\alpha = 0.5$ , and  $\beta = 0.75$ . Although these values are considered in this study for fixed-based frames, the *IMs* for the base-isolated frames (as mentioned previously) are modified by substituting  $T_{ip}$  for  $T_1$ ,  $0.5T_{ip}$  for  $T_2$ , and  $C = 1.25$ .

## 2.2 Vector-valued IMs

Four different vector-valued *IMs* are considered herein which are as follows:

- (a)  $[PGA, M]$  where  $M$  is the moment magnitude of the event generating the ground motion (Elefante et al. 2010). It is expected that this vector is a better predictor than *PGA* alone.
- (b)  $[Sa(T_1), R_{T_1, T^*}]$  where  $R_{T_1, T^*} = Sa(T^*)/Sa(T_1)$ , and  $T^*$  is another period chosen to capture important characteristics of the spectrum’s shape. Depending upon whether  $T^*$  is smaller or larger than  $T_1$ , this vector *IM* is able to provide information about excitation of higher modes or nonlinear response, respectively. Therefore, two values are taken for  $T^*$ ,  $T_1^* = 2T_1$  and  $T_2^* = T_2$ , which was suggested by Baker and Cornell (2008a) as an intuitive choice that agrees reasonably with their results. In a comparative study by Baker and Cornell (2008b), they demonstrated that  $2T_1$  accounts also for the effect of velocity pulses in pulse-like ground motions with  $T_p/T_1 > 2$  where  $T_p$  denotes the measured pulse period. In an attempt to account for pulses that affect higher-mode response, i.e. those with  $0.5 < T_p/T_1 < 1.5$ , consideration was given to the choice  $T_1/3$  (which is approximately equal to  $T_2$  for medium-rise buildings). In case of base-isolated structure,  $T_{ip}$  is used in place of  $T_1$ , and  $T_1^* = 1.25T_{ip}$  and  $T_2^* = 0.5T_{ip}$ .

- (c)  $[Sa(T_1), \varepsilon(T_1)]$  where  $\varepsilon$  is another measure for spectral shape (see Baker and Cornell 2006) defined as the number of standard deviations by which a given  $\ln Sa(T_1)$  value differs from the mean predicted  $\ln Sa(T_1)$  value for a given magnitude  $M$ , distance  $R$ , and other site-source properties denoted as  $\varphi$ . Mathematically, this is written as:

$$\varepsilon(T_1) = \frac{\ln Sa(T_1) - \mu_{\ln Sa(T_1)}(M, R, \varphi)}{\sigma_{\ln Sa(T_1)}(M, R, \varphi)} \tag{5}$$

where  $\mu_{\ln Sa(T_1)}$  and  $\sigma_{\ln Sa(T_1)}$  are the predicted mean and standard deviation, respectively, of  $\ln Sa$  at the given period  $T_1$ . In this study, Campbell and Bozorgnia (2008) (referred as CB08 hereafter) ground-motion prediction equation is used for estimating mean and standard deviation of  $\ln Sa(T_1)$ . In order to account for pulse-like features while the suit of ground motions encounter observed pulses, the predicted mean and standard deviation of  $\ln Sa(T_1)$  at the site are modified according to the observed pulses according to the provisions made by Shahi and Baker (2011) as follows:

$$\begin{aligned} \mu_{\ln Sa(T_1), \text{pulse}} &= \mu_{\ln Af} + \mu_{\ln Sa(T_1)} \\ \sigma_{\ln Sa(T_1), \text{pulse}} &= Rf \cdot \sigma_{\ln Sa(T_1)} \end{aligned} \tag{6}$$

where  $\mu_{\ln Sa(T_1), \text{pulse}}$  and  $\sigma_{\ln Sa(T_1), \text{pulse}}$  are the predicted values of the ground motion model in the presence of pulses, and  $\mu_{\ln Af}$  is its predicted mean value of the amplification factor  $Af$  which allows to model the amplification due to the pulse-like feature. In addition,  $Rf$  is the reduction in standard deviation since the modified ground-motion model for pulse-like ground motions is expected to be lower than the standard deviation of the entire ground-motion library, which contains both pulse-like and non-pulselike ground motions. The following mean amplification function and reduction factor are proposed (see Shahi and Baker 2011):

$$\mu_{\ln Af} = \begin{cases} 1.131 \exp(-3.11 [\ln(T/T_p) + 0.127]^2) + 0.058 & \text{if } T \leq 0.88T_p \\ 0.896 \exp(-2.11 [\ln(T/T_p) + 0.127]^2) + 0.255 & \text{if } T > 0.88T_p \end{cases} \tag{7}$$

$$Rf = \begin{cases} 1 - 0.20 \exp(-0.96 [\ln(T/T_p) + 1.56]^2) & \text{if } T \leq 0.21T_p \\ 1 - 0.21 \exp(-0.24 [\ln(T/T_p) + 1.56]^2) & \text{if } T > 0.21T_p \end{cases} \tag{8}$$

- (d)  $[Sa(T_1), R_{T_1, T^*}, \varepsilon(T_1)]$  is a triple vector which can account for the spectral shape by considering both  $R_{T_1, T^*}$  and  $\varepsilon$ . Baker and Cornell (2008a) revealed that  $R_{T_1, T^*}$  does not fully account for the effect of  $\varepsilon$ . They investigated that neglecting  $\varepsilon$  results in conservative estimates of the demand hazard, especially at large levels of structural response.

### 2.3 Demand parameters

Alternative peak-related demand parameters (i.e.,  $D$ 's) are considered for fixed-base and base-isolated structure as outlined in Table 3.

It is noteworthy that structural damage is reflected not only from maximum deformations or accelerations, but also by the amount of dissipated energy due to cyclic loading



**Table 2** Demand parameters considered in this study

Notation	Name	Structure type	Definition
<i>MRDR</i>	Maximum roof drift ratio	Fixed-base Base-isolated	The ratio of the peak lateral roof displacement (with respect to the base) to the building height/well correlated with the overall structural damage and global instability
<i>MIDR</i>	Maximum inter-story drift ratio	Fixed-base Base-isolated	The maximum value of the peak inter-story drift ratio (drift normalized by the story height) over all stories/closely related to local damage, instability, and story collapse
<i>MFA</i>	Maximum floor acceleration	Fixed-base Base-isolated	The maximum value of the peak floor absolute acceleration over all stories/reflects the level of non-structural damage
<i>MBD</i>	Maximum bearing displacement	Base-isolated	It is a key index for base-isolated structures as a measure of damage at the base level

(cumulative damage). The energy-based demand parameters (see e.g. Benavent-Climent et al. 2002, López-Almansa et al. 2013) such as the normalized hysteretic energy, or the ratio of normalized hysteretic energy to normalized maximum displacement (also known as equivalent number of cycles) are then of major importance to be considered. In fact, they can be more effective than the displacement-based demand parameters especially in building designed according to old codes. However, energy-based demand parameters are not considered in this study (Table 2).

### 3 Methodology

#### 3.1 Efficiency of an IM

This study benefits considerably from an efficient nonlinear dynamic procedure referred to as the *cloud analysis method* (Jalayer and Cornell 2003; Jalayer et al. 2015). The cloud method can be employed in order to quantify the efficiency as well as the relative sufficiency of various *IMs*. The *IM* of interest is assumed to be, in general, a vector of  $m$  variables, i.e.  $\mathbf{IM} = \{IM_i, i = 1:m\}$ . Accordingly, the structure is first subjected to a suite of  $n$  ground-motion wave-forms, and the associated structural response parameters is denoted as  $D = \{y_k, k = 1:n\}$ . By performing a multivariate linear regression in the logarithmic space on  $D$  versus the candidate  $\mathbf{IM}$ , the statistical parameters corresponding to the lognormal distribution of  $D|\mathbf{IM}$  can be extracted. The expected value is modeled as follows:

$$\mathbb{E}[\ln D|\mathbf{IM}] = \ln \eta_{D|\mathbf{IM}} = b_0 + b_1 \ln IM_1 + b_2 \ln IM_2 + \cdots + b_m \ln IM_m \quad (9)$$

where  $\eta_{D|\mathbf{IM}}$  is the conditional median, and the parameters  $b_0$  and  $b_i, i = 1, \dots, m$ , are the estimated regression coefficients. It is to note that Eq. (9) can have options where an  $IM_i, i = 1:m$ , is arithmetic (i.e.,  $IM_i$  instead of  $\ln IM_i$ ). The standard deviation is estimated by the standard error of the regression as:

$$\sigma_{\ln D|\mathbf{IM}} = \beta_{D|\mathbf{IM}} \approx \sqrt{\frac{\sum_{k=1}^n (\ln y_k - \ln \eta_{D|\mathbf{IM}}(\mathbf{IM}_k))^2}{n - (m + 1)}} \tag{10}$$

where  $\sigma_{\ln D|\mathbf{IM}}$  is the conditional standard deviation (or equivalently  $\beta_{D|\mathbf{IM}}$  known as dispersion). It is obvious that in case of having scalar *IMs*, a simple logarithmic linear regression model can be applied (i.e.,  $m = 1$ ). As a result, the cloud analysis implements the non-linear dynamic analysis results in a (linear) regression-based probabilistic model. The estimated dispersion  $\beta_{D|\mathbf{IM}}$  serves as quantitative measure for predictive efficiency of the candidate *IMs*; for instance, those resulting in standard errors in order of 0.20–0.30 are normally considered as those having a proper efficiency, while the range 0.30–0.40 is still considered as reasonably acceptable (see Mollaioli et al. 2013).

Another predictor that used herein for finding how well the sample regression line fits the data is called *coefficient of determination* or the *R-square* ( $R^2$ ). This coefficient provides a relative measure (in percent) of the reduction in standard deviation due to the regression with respect to the marginal standard deviation of the dependent variable (herein,  $D$ ). It is always between zero and one; an *R-square* equal to zero indicates zero reduction in variance with respect to that of the dependent data (very inefficient) and an  $R^2$  equal to 1 indicates 100 % reduction in variance due to regression (very efficient). Accordingly, the *IM* that best predicts the  $D$  is the one that provides the largest value of the  $R^2$  (around 1) among those considered.

### 3.2 Sufficiency of an IM

An **IM** is sufficient in its absolute sense if and only if the probability distribution for demand parameter  $D$  given **IM** is independent of the ground motion acceleration wave-forms denoted as  $\mathbf{a}_g$ :

$$p_{D|\mathbf{IM},\mathbf{a}_g}(y|\mathbf{IM}(\mathbf{a}_g), \mathbf{a}_g) = p_{D|\mathbf{IM}}(y|\mathbf{IM}(\mathbf{a}_g)) \tag{11}$$

That is, knowing **IM**, there is no additional information that can be provided by the ground motion wave-form,  $\mathbf{a}_g$ , necessary for prediction of demand  $D$ .<sup>1</sup> This is clearly a very strong condition, and it is unlikely that any scalar or low-dimensional vector *IM* satisfies it. Furthermore, even if the equality holds for a certain *IM*, it is not at all straightforward to demonstrate that it holds. In order to overcome this obstacle, it seems definitely simpler to talk about the relative sufficiency of one **IM** with respect to another. In this regard, Jalayer et al. 2012 have used the concept of the *relative entropy*, also known as the Kullback–Leibler divergence (Kullback and Leibler 1951) in order to propose a measure of relative sufficiency of one **IM** with respect to another. The relative entropy provides the means of measuring the “distance” between two probability distributions.

The relative entropy  $\mathcal{D}(p_{D|\mathbf{a}_g}||p_{D|\mathbf{IM}})$  between the two probability density functions (PDF)  $p_{D|\mathbf{a}_g}$  and  $p_{D|\mathbf{IM}}$  can be calculated as:

<sup>1</sup> Note that the *IM* itself is a function of the ground motion wave-form  $\mathbf{a}_g$  (as reported in this equation for completeness). However, later on we have dropped out this functional dependence on  $\mathbf{a}_g$  for brevity.

$$\mathcal{D}(p_{D|\mathbf{a}_g} \| p_{D|\mathbf{IM}}) = \int_{\Omega_D} p_{D|\mathbf{a}_g}(y|\mathbf{a}_g) \log_2 \frac{p_{D|\mathbf{a}_g}(y|\mathbf{a}_g)}{p_{D|\mathbf{IM}}(y|\mathbf{IM}(\mathbf{a}_g))} dy \tag{12}$$

Note that the relative entropy  $\mathcal{D}(p_{D|\mathbf{a}_g} \| p_{D|\mathbf{IM}})$  in Eq. (12) is calculated as the expected value of *information gain* or *entropy* between the two PDF’s  $p_{D|\mathbf{a}_g}$  and  $p_{D|\mathbf{IM}}$  (measured in “bits” of information). In other words,  $\mathcal{D}(p_{D|\mathbf{a}_g} \| p_{D|\mathbf{IM}})$  measures on average how much information is lost about demand  $D$  by adopting the intensity measure  $\mathbf{IM}$  instead of the entire ground motion wave-form  $\mathbf{a}_g$ . Based on this definition, the difference in relative entropies  $\mathcal{D}(p_{D|\mathbf{a}_g} \| p_{D|\mathbf{IM}_1})$  and  $\mathcal{D}(p_{D|\mathbf{a}_g} \| p_{D|\mathbf{IM}_2})$  can be written as:

$$\mathcal{D}(p_{D|\mathbf{a}_g} \| p_{D|\mathbf{IM}_1}) - \mathcal{D}(p_{D|\mathbf{a}_g} \| p_{D|\mathbf{IM}_2}) = \int_{\Omega_D} p_{D|\mathbf{a}_g}(y|\mathbf{a}_g) \log_2 \frac{p_{D|\mathbf{IM}_2}(y|\mathbf{IM}_2(\mathbf{a}_g))}{p_{D|\mathbf{IM}_1}(y|\mathbf{IM}_1(\mathbf{a}_g))} dy \tag{13}$$

Jalayer et al. (2012) have defined the relative sufficiency of two alternative *IMs*,  $\mathbf{IM}_1$  and  $\mathbf{IM}_2$  as the expected value of their relative entropies defined in Eq. (13) over all possible ground motion waveforms.

$$I(D|\mathbf{IM}_2|\mathbf{IM}_1) = \int_{\Omega_{\mathbf{a}_g}} \left[ \int_{\Omega_D} p_{D|\mathbf{a}_g}(y|\mathbf{a}_g) \log_2 \frac{p_{D|\mathbf{IM}_2}(y|\mathbf{IM}_2(\mathbf{a}_g))}{p_{D|\mathbf{IM}_1}(y|\mathbf{IM}_1(\mathbf{a}_g))} dy \right] p_{\mathbf{a}_g}(\mathbf{a}_g) d\mathbf{a}_g \tag{14}$$

For a given  $\mathbf{a}_g$ ,  $y$  is known and is equal to  $y(\mathbf{a}_g)$ ; hence, the probability  $p_{D|\mathbf{a}_g}$  reduces to the Dirac delta function  $\delta[y(\mathbf{a}_g)]$ . Therefore, the equation can further be simplified as:

$$\begin{aligned} I(D|\mathbf{IM}_2|\mathbf{IM}_1) &= \int_{\Omega_{\mathbf{a}_g}} \left[ \int_{\Omega_D} \delta(y(\mathbf{a}_g)) \log_2 \frac{p_{D|\mathbf{IM}_2}(y|\mathbf{IM}_2(\mathbf{a}_g))}{p_{D|\mathbf{IM}_1}(y|\mathbf{IM}_1(\mathbf{a}_g))} dy \right] p_{\mathbf{a}_g}(\mathbf{a}_g) d\mathbf{a}_g \\ &= \int_{\Omega_{\mathbf{a}_g}} \log_2 \frac{p_{D|\mathbf{IM}_2}(y(\mathbf{a}_g)|\mathbf{IM}_2(\mathbf{a}_g))}{p_{D|\mathbf{IM}_1}(y(\mathbf{a}_g)|\mathbf{IM}_1(\mathbf{a}_g))} p_{\mathbf{a}_g}(\mathbf{a}_g) d\mathbf{a}_g \end{aligned} \tag{15}$$

If  $I(D|\mathbf{IM}_2|\mathbf{IM}_1)$  is positive, this means that on average  $\mathbf{IM}_2$  provides more information about  $D$  than  $\mathbf{IM}_1$ ; hence,  $\mathbf{IM}_2$  is more sufficient than  $\mathbf{IM}_1$ . Similarly, if  $I(D|\mathbf{IM}_2|\mathbf{IM}_1)$  is negative,  $\mathbf{IM}_2$  is less sufficient than  $\mathbf{IM}_1$ . Jalayer et al. (2012) proposed a refined method for calculating the integral in Eq. (15) through Monte Carlo Simulation by adopting a stochastic ground motion model in conjunction with deaggregation of the seismic hazard at the site. In addition, they argued that the relative sufficiency measure (RSM) can be approximately calculated by replacing the expectation with an average over a suite of  $n$  real ground motion records:

$$I(D|\mathbf{IM}_2|\mathbf{IM}_1) \approx \frac{1}{n} \sum_{k=1}^n \log_2 \frac{p_{D|\mathbf{IM}_2}(y_k|\mathbf{IM}_2)}{p_{D|\mathbf{IM}_1}(y_k|\mathbf{IM}_1)} \tag{16}$$

where  $D = \{y_k, k = 1:n\}$  are the demand values for a suite of  $n$  ground motions (obtained from cloud analysis, see Sect. 3.1). This provides a preliminary ranking of candidate  $\mathbf{IM}_2$  with respect to the reference  $\mathbf{IM}_1$ . Although the simplified and approximate formulation in Eq. (16) offers an efficient solution for comparing various *IMs* without the need to use a

stochastic ground motion model, it may yield inaccurate results<sup>2</sup> (see also Jalayer et al. 2012).

The probability distribution function (PDF)  $p_{D|\mathbf{IM}}(y|\mathbf{IM})$  can be calculated by considering a lognormal distribution with the parameters defined in Eqs. (9) and (10):

$$p_{D|\mathbf{IM}}(y|\mathbf{IM}) = \frac{1}{y\beta_{D|\mathbf{IM}}} \phi\left(\frac{\ln y - \ln \eta_{D|\mathbf{IM}}}{\beta_{D|\mathbf{IM}}}\right) \quad (17)$$

where  $\phi(\cdot)$  is the standardized Gaussian PDF. Hence, the relative sufficiency measure can approximately be expressed as:

$$I(D|\mathbf{IM}_2|\mathbf{IM}_1) \approx \frac{1}{n} \sum_{k=1}^n \log_2 \left( \frac{\beta_{D|\mathbf{IM}_1} \phi\left(\frac{\ln y_k - \ln \eta_{D|\mathbf{IM}_2}(\mathbf{IM}_{2,k})}{\beta_{D|\mathbf{IM}_2}}\right)}{\beta_{D|\mathbf{IM}_2} \phi\left(\frac{\ln y_k - \ln \eta_{D|\mathbf{IM}_1}(\mathbf{IM}_{1,k})}{\beta_{D|\mathbf{IM}_1}}\right)} \right) \quad (18)$$

## 4 Numerical example

### 4.1 Ground motion database

In this study, 137 earthquake ground motions are selected from the next generation of attenuation (NGA) database (Chiou et al. 2008), and used as input for the cloud analysis methodology. The suite of wave-forms is divided into two subsets: (1) 78 ordinary ground motions with closest distance and magnitude ranging  $0.64 \text{ km} \leq R_{\text{rup}} \leq 87.87 \text{ km}$ , and  $5.74 \leq M \leq 7.90$ , respectively; (2) 56 pulse-like near-fault ground motions with  $0.07 \text{ km} \leq R_{\text{rup}} \leq 20.82 \text{ km}$  and  $5.0 \leq M \leq 7.62$ . Selected records are predominantly on soil type C or D according to the NEHRP site classification based on the preferred  $V_{s30}$  values. It is noteworthy that current database is the one used previously by Mollaioli et al. (2013) with minor modifications implemented herein. Accordingly, ordinary ground motions are selected from one of the components of the corresponding NGA earthquakes while pulse-like ones are the specifically fault-normal rotated orientation of the two orthogonal components.

This classification of NGA records as pulse-like is originally based on the automated algorithm proposed by Baker (2007) which identifies pulse-like records using wavelet transforms. This algorithm uses the fault-normal component of ground motion for its classification. Nevertheless, pulses are often found in other orientations due to complex geometry of a real fault; thus, the velocity pulse can be present in orientations other than the computed fault-normal orientation. For this purpose, Shahi (2013) proposed an efficient algorithm that can acquire pulses at arbitrary orientations in multi-component ground motions. Based on this new algorithm, 44 out of 56 fault-normal components presented by Mollaioli et al. (2013) are classified as pulse-like ground motions. The details of each recording in both ordinary and pulse-like ground-motion sets together with the plot of their spectral accelerations are reported in the Appendix of the paper available as Online Resource.

<sup>2</sup> This is to be expected since estimating the integral in Eq. (15) using a small-size set of records not only implies that  $p(\mathbf{a}_g)$  is estimated by a uniform discrete probability distribution, but also it estimates the record-to-record variability by what is depicted from a small sample of records.

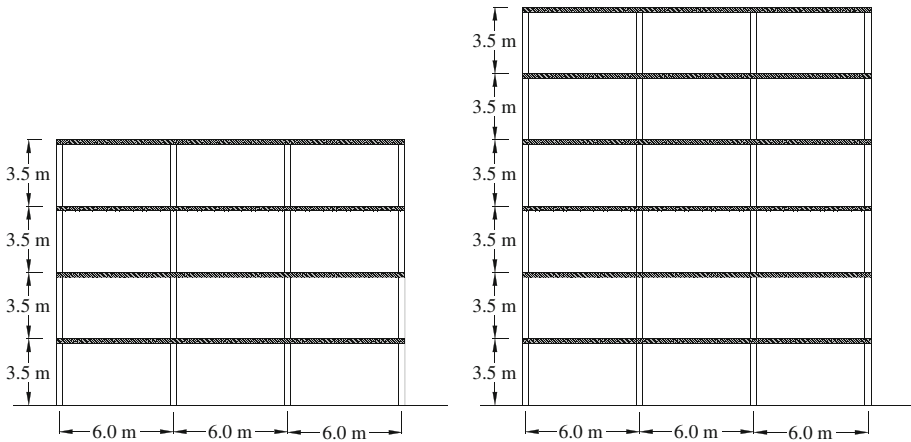


**Fig. 2** Schematic representation of the case-study RC frame structures

**Table 3** Periods of the first three modes of vibration of the fixed-base frames

Frame	Fixed-base		Base-isolated	
	$T_1$ (s)	$T_2$ (s)	$T_3$ (s)	$T_{ip}$ (s)
4-Story	0.97	0.33	0.20	2.5
6-Story	1.17	0.40	0.24	3.0

### 4.2 Description of case-study buildings

The case-study buildings are two three-bay 2-dimensional RC frames consisting of 4-story and 6-story structures dimensioned according to an Italian former code (DM 96, 1996), which lacks in specific capacity design rules. They are representative of existing buildings located in high seismic zones (i.e., “zone 1” according to the seismic hazard classification of DM 96). A schematic representation of the two frames is illustrated in Fig. 2 (for more details about the building structures, see Mollaioli et al. 2013). The periods of the first three modes of vibration of the fixed-base frames, obtained with a reduced cracked stiffness of the structural elements equal to half the initial elastic ones, are outlined in Table 3.

The required non-linear dynamic analyses for the cloud analysis procedure are performed in OpenSees 2.2.2 (2010). The physical models of the two structures are built using Beam with Fibre-Hinges Elements for modelling beams and columns of the frames. The masses are concentrated at the nodes, and the stiffness of the floors is modelled with rigid diaphragm constraints. A Rayleigh damping proportional to the mass and tangent stiffness matrix is used, with coefficients calibrated to provide a 5 % damping at the first and second mode periods of the undamaged structures. The effects of geometric nonlinearities are not considered in the analyses.

In order to study the base-isolated systems in addition to ordinary fixed-based buildings, the same frames equipped with four different isolation properties are used in this study (see Mollaioli et al. 2013; Fig. 2). The considered isolation systems have bi-linear backbone curves with positive post-yield stiffness ratio and no stiffness degradation under cyclic loadings. To characterize four different isolation systems, the parameters of the backbone curve are defined as follows: (1) the characteristic strength is set  $F_d = 0.03 W$  where W is the

seismic weight of the corresponding structure; (2) the elastic limit displacement is  $D_y = \{0, 10, 25, 50 \text{ mm}\}$ , which are representative of different isolation systems (e.g.,  $D_y = 0$  shows friction pendulum isolators, and  $D_y > 0$  correspond to lead rubber bearings with different initial stiffness); (3) the post-elastic stiffness is set so that the isolation periods  $T_{ip}$  outlined in Table 3 associated with the 4-story and 6-story buildings are attained.

### 4.3 Results in terms of efficiency

The logarithmic standard deviation of regression residuals,  $\beta_{D|IM}$ , as well as the  $R^2$  corresponding to the demand parameters  $MRDR$ ,  $MIDR$  and  $MFA$  are obtained from the regression model (see Sect. 3.1) for both case-study fixed-base buildings (Fig. 3) and base-isolated buildings equipped with the isolation system having  $D_y = 10 \text{ mm}$  (Fig. 4). The structures are subjected to both ordinary and pulse-like ground motions. The efficiency results are illustrated in those figures for all 38  $IMs$  (i.e., 32 scalar and 6 vector-valued). For scalar  $IMs$ , as explained formerly in Sect. 3.1, a simple linear regression in the logarithmic scale is performed on  $D$  versus the candidate  $IM$ . However, for the vector-valued  $IMs$  outlined in Table 1, the multi-linear regression models for  $\eta_{D|IM}$ , with reference to Eq. (9), have the following forms:

$$\begin{aligned} \ln \eta_{D|[PGA,M]} &= b_0 + b_1 \ln PGA + b_2 M \\ \ln \eta_{D|[Sa(T_1),R_{T_1},T_1^*]} &= b_0 + b_1 \ln Sa(T_1) + b_2 \ln R_{T_1,T_1^*} \\ \ln \eta_{D|[Sa(T_1),\varepsilon(T_1)]} &= b_0 + b_1 \ln Sa(T_1) + b_2 \varepsilon(T_1) \\ \ln \eta_{D|[Sa(T_1),R_{T_1},T_1^*,\varepsilon(T_1)]} &= b_0 + b_1 \ln Sa(T_1) + b_2 \ln R_{T_1,T_1^*} + b_3 \varepsilon(T_1) \end{aligned} \quad (19)$$

According to Figs. 3 and 4, the following general conclusions can be drawn for the fixed-based as well as base-isolated case-study frames:

- The dispersion values obtained from cloud regression for the  $MRDR$  are generally less sensitive to different types of buildings and ground motions with respect to those for  $MIDR$ . Nevertheless, these two demand parameters follow similar trend since inter-story drift demands are distributed almost uniformly within the structural height. This is likely to be interpreted by the fact that although the case-study frames are not ductile as modern designed structures, they are not characterized by any specific irregular behaviour which produces significant localization of seismic damages.
- The  $MRDR$  and  $MIDR$  are more efficiently predicted with ordinary ground motions rather than pulse-like ones. In other words, regression models are better fitted to data from ordinary ground motion set compared to pulse-like ones.
- The demand parameter  $MFA$  follows similar trends regarding different types of buildings and ground motions.
- The structure-specific and vector-valued  $IMs$  are generally more efficient, especially for  $MIDR$ ,  $MRDR$ , and  $MBD$ .
- In predicting the  $MFA$ , both  $PGA$  and modified structure-specific  $IMs$  are more efficient than other considered  $IMs$ . However, the regression models associated with different  $IMs$  are generally less efficient for this demand parameter with respect to the other demand parameters.
- $Sa$  is generally one of the efficient  $IMs$  for predicting  $MRDR$  and  $MIDR$  in fixed-base structures. This fact has been demonstrated by many researchers (see e.g. Shome et al. 1998; Shome and Cornell 1999). However, it does not hold for base-isolated buildings.

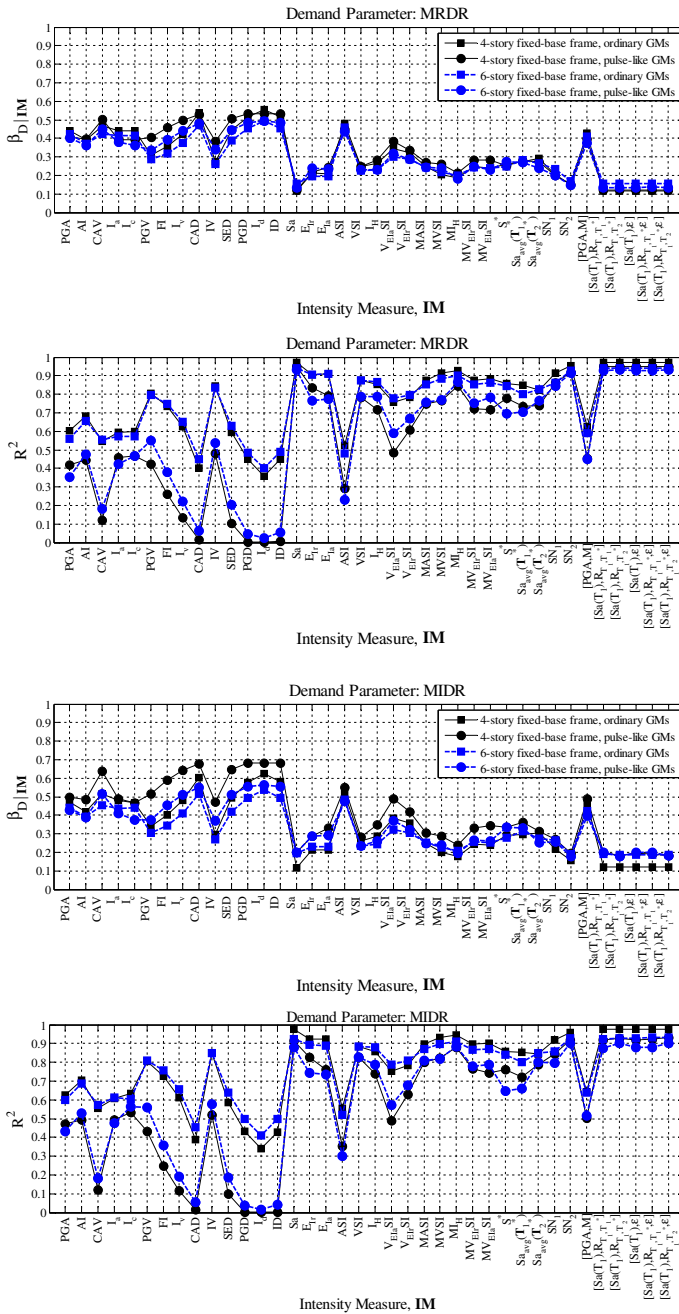


**Fig. 3** Logarithmic standard deviation of regression residuals,  $\beta_{D|IM}$ , and the  $R$ -squared,  $R^2$ , corresponding to the demand parameters *MRDR*, *MIDR* and *MFA*, obtained from the cloud analysis of fixed-base buildings subjected to ordinary and pulse-like ground motions

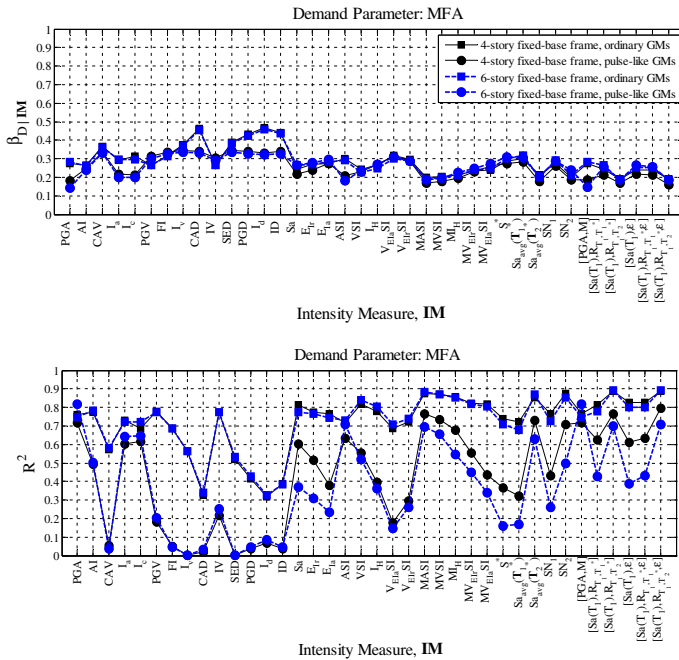
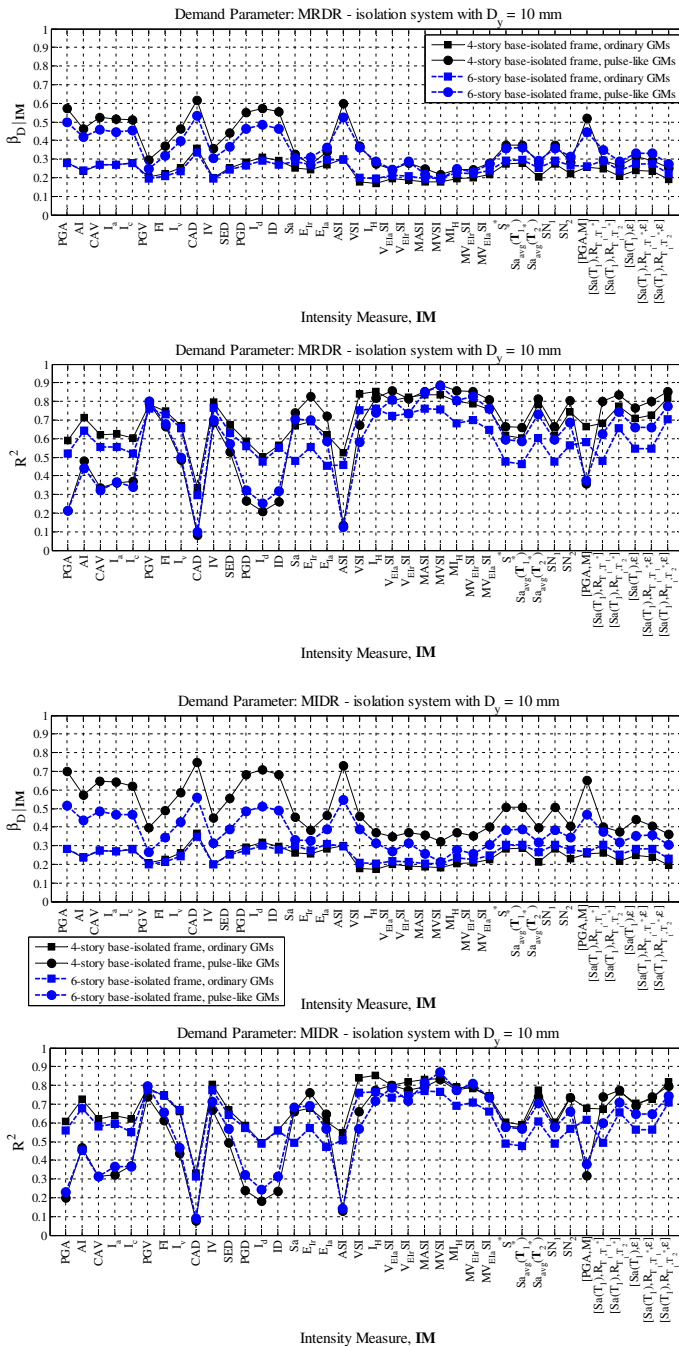


Fig. 3 continued

As an example of finding an efficient *IM*, consider the case of 6-story fixed-base building in Fig. 3 with the set of pulse-like ground motions, and demand parameter *MIDR*. For *IM* = *CAD* (Cumulative Absolute Displacement), the cloud regression is shown in Fig. 5a. It indicates that  $\beta_{D|IM} = 0.55$  ( $>0.40$  according to the limits proposed by Mollaioli et al. 2013) and  $R^2 = 0.054$ . Therefore, *CAD* is not an efficient *IM* for predicting the demand parameter *MIDR* using the proposed regression. On the other hand, for *IM* = *S<sub>N2</sub>* (multi-parameter intensity measure), the cloud regression (illustrated in Fig. 5b) indicates  $\beta_{D|IM} = 0.18$  and  $R^2 = 0.90$ . Hence, this *IM* is efficient in predicting the desired demand parameter. As another example, consider the 4-story base-isolated building with  $D_y = 10$  mm, (see Fig. 4) considering set of ordinary ground motions, and demand parameter *MIDR*. The cloud regression is illustrated in Fig. 6a for *IM* = *CAD* and in Fig. 6b for *IM* = *I<sub>H</sub>* (Housner intensity). Although  $\beta_{D|IM} = 0.37$  for *IM* = *CAD* is within the acceptable range ( $<0.40$ ), the  $R^2$  is too small ( $R^2 = 0.33$ ) and the *IM* is not efficient. This is while *IM* = *I<sub>H</sub>* with  $\beta_{D|IM} = 0.17$  and  $R^2 = 0.85$  is efficient.

One of the objectives herein is to find the most efficient *IMs* (among those outlined in Table 1), which are capable of properly predicting the demand for the existing typical buildings designed according to older Italian building codes. To achieve this goal, the first 6 (in some cases up to 8) most efficient *IMs*, which ensure lowest  $\beta_{D|IM}$  and highest  $R^2$  (as explained in the above paragraphs), are selected. These *IMs* are tabulated for alternative demand parameters in Table 4 and Tables 5, 6, 7 and 8 corresponding to fixed-base and base-isolated building (equipped with four different isolation systems defined in previous section), respectively. The selection of the most efficient *IMs* is performed individually for the set of ordinary and pulse-like ground motions. It is worth noting that the orders of *IMs* in those Tables are compatible with their layout shown in Table 1.





**Fig. 4** Logarithmic standard deviation of regression residuals,  $\beta_{D|IM}$ , and the R-squared,  $R^2$ , corresponding to the demand parameters MRDR, MIDR, MBD, and MFA, obtained from the cloud analysis of base-isolated buildings equipped with isolation system having  $D_y = 10$  mm, subjected to ordinary and pulse-like ground motions

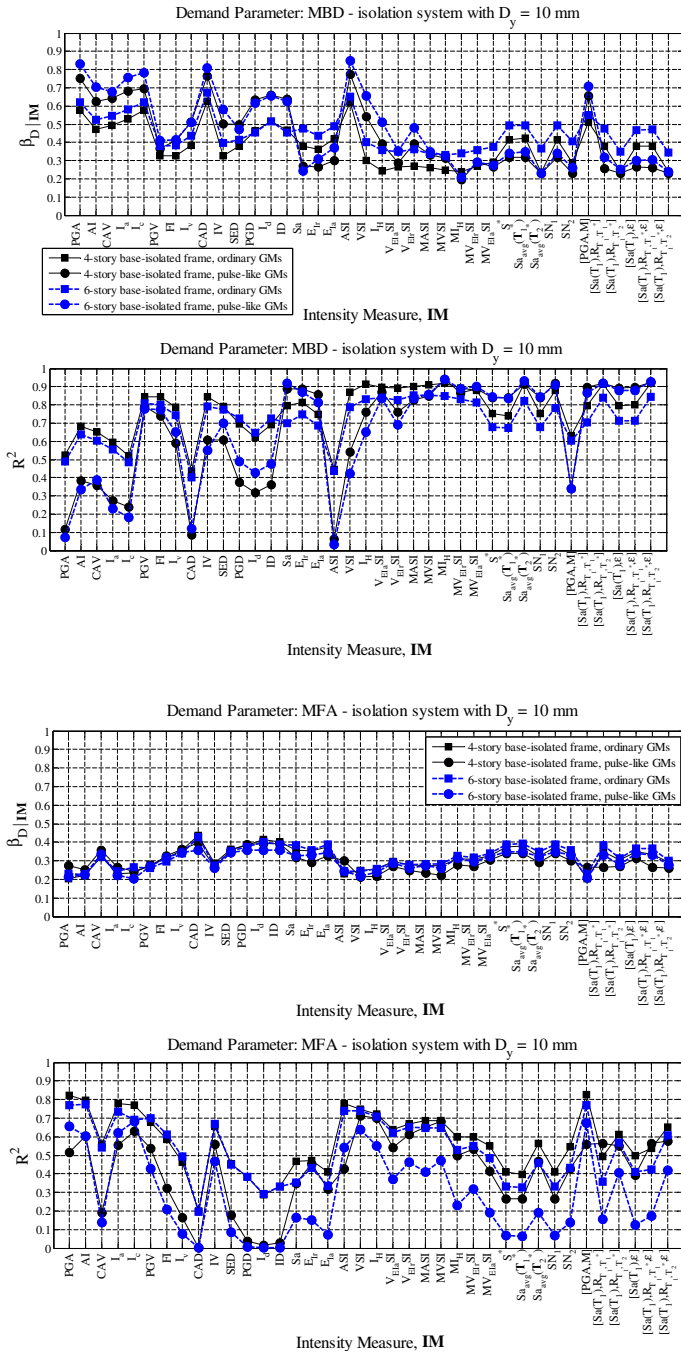
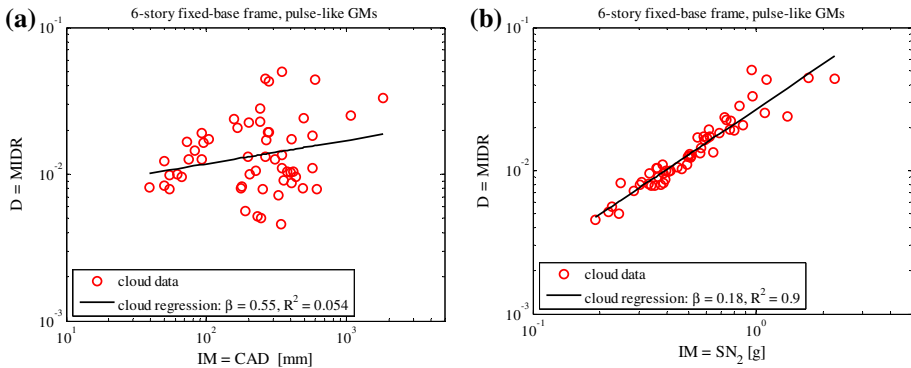


Fig. 4 continued



**Fig. 5** Comparison of cloud regression plots of alternative *IMs* **a** *CAD*, and **b** *S<sub>N2</sub>*

With reference to Table 4 for fixed-based structures, it is particularly observed that:

- For demand parameters *MRDR* and *MIDR*, modified integral intensity  $MI_H$  (modified Housner intensity), the multi-parameter intensity  $S_{N2}$ , and all the suggested vector-valued *IMs*, except for [*PGA*, *M*], are all efficient with respect to the spectral acceleration at the first-mode period  $S_a$ , considering different sets of ground-motions.
- For demand parameter *MFA*, modified integral intensities *MASI* (modified acceleration spectrum intensity), and *MAVI* (modified velocity spectrum intensity), as well as the multi-parameter intensity  $S_{a_{avg}}(\mathbf{T}_2^*)$  accounting for higher-mode effect are efficient for different sets of ground-motions.
- The scalar intensity *PGA* and the vector-valued [*PGA*, *M*] are sensitive to pulse-like ground motions for predicting the demand parameter *MFA*.
- Generally speaking, the vector-valued intensities [ $S_a(T_1), R_{T_1, T_2^*}$ ] and [ $S_a(T_1), R_{T_1, T_2^*}, \varepsilon$ ], which account for higher-mode effect, are efficient with respect to all considered demand parameters.

With reference to Tables 5, 6, 7 and 8 for base-isolated frames, the following conclusions can be drawn:

- For *MRDR* and *MIDR*, quite the same trend in efficient *IMs* is shown among different isolation systems; that is, the set of integral *IMs* comprising  $V_{Ela}SI$ ,  $V_{EIr}SI$ , *MASI*, *MVSI*,  $I_H$ ,  $MI_H$ ,  $MV_{EIr}SI$  (refer to Table 1 for their corresponding definitions) are proper *IMs* for predicting the aforementioned peak-related demand parameters regarding different set of ground-motions. Moreover, the vector-valued intensity [ $S_a(T_1), R_{T_1, T_2^*}, \varepsilon$ ] which account for both the spectral shape and the higher-mode effect is very efficient with respect to pulse-like ground-motions.
- For *MBD*, the list of efficient *IMs* is independent of the type of isolation system (i.e.,  $D_y$ ) for the pulse-like ground-motion set; this is mainly for the reason that these records provide high bearing displacements. Moreover, as the yield displacement of the isolation system increases, the list of efficient *IMs* for the ordinary ground-motion set resembles more and more that of the pulse-like set. As a result, the modified integral intensity  $MI_H$ , the multi-parameter intensity  $S_{a_{avg}}(\mathbf{T}_2^*)$ , as well as the vector-valued intensities [ $S_a(T_1), R_{T_1, T_2^*}$ ], and [ $S_a(T_1), R_{T_1, T_2^*}, \varepsilon$ ] are efficient in case of *MBD* for various isolation systems and ground-motion sets.

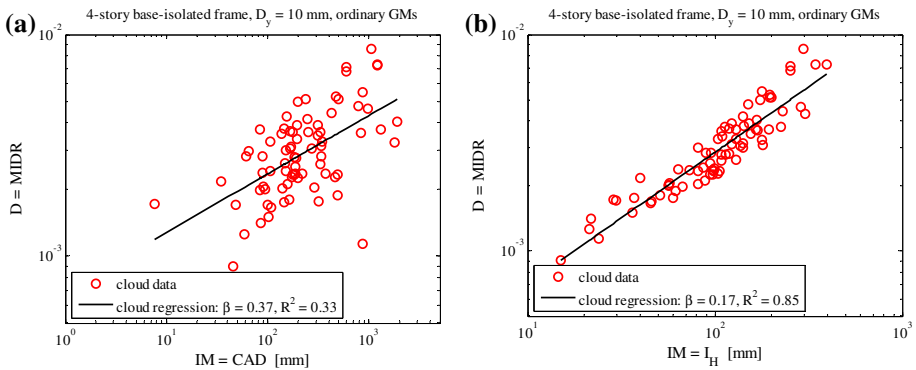


**Fig. 6** Comparison of cloud regression plots of alternative *IMs* **a** *CAD*, and **b** *I<sub>H</sub>*

**Table 4** The most efficient *IMs* for fixed-base case-study buildings

<i>MRDR</i>		<i>MIDR</i>		<i>MFA</i>	
Ordinary	Pulse-like	Ordinary	Pulse-like	Ordinary	Pulse-like
<i>S<sub>a</sub></i>	<i>S<sub>a</sub></i>	<i>S<sub>a</sub></i>	<i>S<sub>a</sub></i>	<i>MASI</i>	<i>PGA</i>
<i>MI<sub>H</sub></i>	<i>MI<sub>H</sub></i>	<i>MI<sub>H</sub></i>	<i>MI<sub>H</sub></i>	<i>MVSI</i>	<i>MASI</i>
<i>S<sub>N2</sub></i>	<i>S<sub>N2</sub></i>	<i>S<sub>N2</sub></i>	<i>S<sub>N2</sub></i>	<i>MI<sub>H</sub></i>	<i>MVSI</i>
$[S_a(T_1), R_{T_1, T_1^*}]$	$[S_a(T_1), R_{T_1, T_1^*}]$	$[S_a(T_1), R_{T_1, T_1^*}]$	$[S_a(T_1), R_{T_1, T_1^*}]$	$S_{avg}(T_2^*)$	$S_{avg}(T_2^*)$
$[S_a(T_1), R_{T_1, T_2^*}]$	$[S_a(T_1), R_{T_1, T_2^*}]$	$[S_a(T_1), R_{T_1, T_2^*}]$	$[S_a(T_1), R_{T_1, T_2^*}]$	<i>S<sub>N2</sub></i>	$[PGA, M]$
$[S_a(T_1), \varepsilon]$	$[S_a(T_1), \varepsilon]$	$[S_a(T_1), \varepsilon]$	$[S_a(T_1), \varepsilon]$	$[S_a(T_1), R_{T_1, T_2^*}]$	$[S_a(T_1), R_{T_1, T_2^*}]$
$[S_a(T_1), R_{T_1, T_1^*}, \varepsilon]$	$[S_a(T_1), R_{T_1, T_1^*}, \varepsilon]$	$[S_a(T_1), R_{T_1, T_1^*}, \varepsilon]$	$[S_a(T_1), R_{T_1, T_1^*}, \varepsilon]$	$[S_a(T_1), R_{T_1, T_2^*}, \varepsilon]$	$[S_a(T_1), R_{T_1, T_2^*}, \varepsilon]$
$[S_a(T_1), R_{T_1, T_2^*}, \varepsilon]$	$[S_a(T_1), R_{T_1, T_2^*}, \varepsilon]$	$[S_a(T_1), R_{T_1, T_2^*}, \varepsilon]$	$[S_a(T_1), R_{T_1, T_2^*}, \varepsilon]$		

- For *MFA*, the same trend (approximately) is observed among different isolation systems. As a result, the non-structure-specific *IMs* comprising of *PGA*, *AI*, *I<sub>a</sub>*, *I<sub>c</sub>* (see Table 1 for their corresponding definitions), the integral intensities *ASI*, *VSI*, and *I<sub>H</sub>*, and finally the vector  $[PGA, M]$  are the most efficient ones.
- With reference to the all previous observations, the modified integral intensity *MI<sub>H</sub>* and the vector-valued intensity  $[S_a(T_1), R_{T_1, T_2^*}, \varepsilon]$  are consistently efficient for displacement-based demand parameters and both types of fixity conditions. For the acceleration-based demand parameter *MFA*, the scalar intensity *PGA* and the vector  $[PGA, M]$  are commonly efficient.

An important issue that is raised while comparing the efficiency of various *IMs* associated with the pulse-like records, is mainly related to the pulse period *T<sub>p</sub>*. Short-period pulses with small *T<sub>p</sub>/T<sub>1</sub>* ratio (i.e. < 1–1.5) are capable for affecting the structures for which the higher modes of vibration are contributing significantly to the response. Conversely, records with higher *T<sub>p</sub>/T<sub>1</sub>* values control the peak displacements associated with the first-mode dominant structures (see also Baker and Cornell 2008a). This issue can affect the regression models associated with multi-parameter as well as vector-valued *IMs*

**Table 5** The most efficient *IMs* for base-isolated case-study buildings with  $D_y = 0$  mm

<i>MRDR</i>		<i>MIDR</i>		<i>MBD</i>		<i>MFA</i>	
Ordinary	Pulse-like	Ordinary	Pulse-like	Ordinary	Pulse-like	Ordinary	Pulse-like
<i>VSI</i>	$V_{ElaSI}$	<i>VSI</i>	$V_{ElaSI}$	<i>PGV</i>	$MI_H$	<i>PGA</i>	<i>PGA</i>
$I_H$	<i>MASI</i>	$I_H$	<i>MASI</i>	<i>FI</i>	$MV_{ElaSI}$	<i>AI</i>	<i>AI</i>
$V_{EIrSI}$	<i>MVSI</i>	$V_{EIrSI}$	<i>MVSI</i>	<i>IV</i>	$Sa_{avg}(T_2^*)$	$I_a$	$I_a$
$V_{ElaSI}$	$MI_H$	$V_{ElaSI}$	$MI_H$	$I_H$	$S_{N2}$	$I_c$	$I_c$
<i>MASI</i>	$MV_{EIrSI}$	<i>MASI</i>	$MV_{EIrSI}$	<i>MASI</i>	$[Sa(T_1), R_{T_1, T_2}]$	<i>ASI</i>	<i>ASI</i>
<i>MVSI</i>	$[Sa(T_1), R_{T_1, T_2}, \varepsilon]$	<i>MVSI</i>	$[Sa(T_1), R_{T_1, T_2}, \varepsilon]$	<i>MVSI</i>	$[Sa(T_1), R_{T_1, T_2}, \varepsilon]$	<i>VSI</i>	$[PGA, M]$
				$MI_H$		$I_H$	
						$[PGA, M]$	

**Table 6** The most efficient *IMs* for base-isolated case-study buildings with  $D_y = 10$  mm

<i>MRDR</i>		<i>MIDR</i>		<i>MBD</i>		<i>MFA</i>	
Ordinary	Pulse-like	Ordinary	Pulse-like	Ordinary	Pulse-like	Ordinary	Pulse-like
<i>VSI</i>	$V_{ElaSI}$	<i>VSI</i>	$V_{ElaSI}$	<i>MASI</i>	$MI_H$	<i>PGA</i>	<i>AI</i>
$I_H$	<i>MASI</i>	$I_H$	<i>MASI</i>	<i>MVSI</i>	$MV_{ElaSI}$	<i>AI</i>	$I_c$
$V_{EIrSI}$	<i>MVSI</i>	$V_{EIrSI}$	<i>MVSI</i>	$MI_H$	$Sa_{avg}(T_2^*)$	$I_a$	<i>VSI</i>
$V_{ElaSI}$	$MI_H$	$V_{ElaSI}$	$MI_H$	$[Sa(T_1), R_{T_1, T_2}]$	$S_{N2}$	$I_c$	$I_H$
<i>MASI</i>	$MV_{EIrSI}$	<i>MASI</i>	$MV_{EIrSI}$	$[Sa(T_1), R_{T_1, T_2}, \varepsilon]$	$[Sa(T_1), R_{T_1, T_2}]$	<i>ASI</i>	<i>MVSI</i>
<i>MVSI</i>	$[Sa(T_1), R_{T_1, T_2}, \varepsilon]$	<i>MVSI</i>	$[Sa(T_1), R_{T_1, T_2}, \varepsilon]$		$[Sa(T_1), R_{T_1, T_2}, \varepsilon]$	<i>VSI</i>	
						$I_H$	
						$[PGA, M]$	

(see Table 1). Although these *IMs* are effective for a specific range of periods, the selected set of pulse-like ground-motion comprises records with both ranges of  $T_p/T_1$ . This may reduce the efficiency of the candidate *IMs*. To further study this effect on both fixed-based and base-isolated structures, two subsets of pulse-like records are selected. The pulse-like records with  $T_p/T_1 < 1$  and those with  $T_p/T_1 \geq 1$  are separated from the original set, and the cloud regression is performed separately on either of subsets. This distinction is expected to increase the efficiency of *IMs*.

Figure 7 illustrates  $\beta_{DIIM}$  and  $R^2$  of the regression model for *Sa*, multi-parameter, and vector-valued *IMs* corresponding to the demand parameters *MIDR* associated with the fixed-based structure.

It is observed that for the 6-story building subjected to the set of pulse-like records with  $T_p/T_1 < 1$ , the multi-parameter intensity  $S_{N2}$ , and the vector-valued intensities  $[Sa(T_1), R_{T_1, T_2}]$  and  $[Sa(T_1), R_{T_1, T_2}, \varepsilon]$  have a reduction in  $\beta_{DIIM}$  while their corresponding  $R^2$  remain unchanged. These *IMs*, which are sensitive to higher-mode effect, express higher efficiency with respect to the set of records with  $T_p/T_1 < 1$ . However, the same reasoning does not apply for the 4-story building which is not affected by higher modes. It is to note

**Table 7** The most efficient *IMs* for base-isolated case-study buildings with  $D_y = 25$  mm

<i>MRDR</i>		<i>MIDR</i>		<i>MBD</i>		<i>MFA</i>	
Ordinary	Pulse-like	Ordinary	Pulse-like	Ordinary	Pulse-like	Ordinary	Pulse-like
<i>VSI</i>	$V_{Ela}SI$	<i>VSI</i>	$V_{Ela}SI$	$V_{Ela}SI$	$MI_H$	<i>PGA</i>	<i>VSI</i>
$I_H$	<i>MASI</i>	$I_H$	<i>MASI</i>	$MI_H$	$S_{avg}(\mathbf{T}_2^*)$	<i>AI</i>	$I_H$
$V_{EIr}SI$	<i>MVSI</i>	$V_{EIr}SI$	<i>MVSI</i>	$MV_{EIr}SI$	$S_{N2}$	$I_a$	$V_{EIr}SI$
$V_{Ela}SI$	$MI_H$	$V_{Ela}SI$	$MI_H$	$S_{avg}(\mathbf{T}_2^*)$	$[Sa(T_1), R_{T_1, T_2}]$	<i>ASI</i>	<i>MVSI</i>
<i>MASI</i>	$MV_{EIr}SI$	<i>MASI</i>	$MV_{EIr}SI$	$[Sa(T_1), R_{T_1, T_2}]$	$[Sa(T_1), R_{T_1, T_2}, \varepsilon]$	<i>VSI</i>	
<i>MVSI</i>	$[Sa(T_1), R_{T_1, T_2}, \varepsilon]$	<i>MVSI</i>	$[Sa(T_1), R_{T_1, T_2}, \varepsilon]$	$[Sa(T_1), R_{T_1, T_2}, \varepsilon]$		$I_H$	
							$[PGA, M]$

**Table 8** The most efficient *IMs* for base-isolated case-study buildings with  $D_y = 50$  mm

<i>MRDR</i>		<i>MIDR</i>		<i>MBD</i>		<i>MFA</i>	
Ordinary	Pulse-like	Ordinary	Pulse-like	Ordinary	Pulse-like	Ordinary	Pulse-like
$I_H$	$V_{Ela}SI$	$I_H$	$V_{Ela}SI$	$MI_H$	$MI_H$	<i>PGA</i>	<i>VSI</i>
$V_{EIr}SI$	<i>MASI</i>	$V_{EIr}SI$	<i>MASI</i>	$S_{avg}(\mathbf{T}_2^*)$	$S_{avg}(\mathbf{T}_2^*)$	<i>AI</i>	$I_H$
$V_{Ela}SI$	<i>MVSI</i>	$V_{Ela}SI$	<i>MVSI</i>	$S_{N2}$	$S_{N2}$	$I_a$	$V_{EIr}SI$
<i>MVSI</i>	$MI_H$	<i>MVSI</i>	$MI_H$	$[Sa(T_1), R_{T_1, T_2}]$	$[Sa(T_1), R_{T_1, T_2}]$	<i>ASI</i>	<i>MVSI</i>
$MI_H$	$MV_{EIr}SI$	$MI_H$	$MV_{EIr}SI$	$[Sa(T_1), R_{T_1, T_2}, \varepsilon]$	$[Sa(T_1), R_{T_1, T_2}, \varepsilon]$	<i>VSI</i>	
$MV_{EIr}SI$	$[Sa(T_1), R_{T_1, T_2}, \varepsilon]$	$MV_{EIr}SI$	$[Sa(T_1), R_{T_1, T_2}, \varepsilon]$			$I_H$	
							$[PGA, M]$

that the set of records with  $T_p/T_1 \geq 1$  has no superiority over the original set in terms of efficiency. This is mainly due to the fact that for the set of pulse-like ground motions, the number of records having  $T_p/T_1 \geq 1$  are higher than those with  $T_p/T_1 < 1$ . Therefore, no specific improvement in efficiency can be observed. The same experience is performed on the base-isolated structures with  $D_y = 50$  mm and for the demand parameter *MBD*, as illustrated in Fig. 8. For the 6-story structure, a more pronounced reduction in  $\beta_{DIM}$  is observed with  $R^2$  remaining quite unchanged considering pulse-like records with  $T_p/T_1 > 1$  with respect to the multi-parameter intensities  $S^*$ ,  $S_{avg}(\mathbf{T}_1^*)$ ,  $S_{N1}$ , and vector-valued ones comprising  $[Sa(T_1), R_{T_1, T_1^*}]$ , and  $[Sa(T_1), R_{T_1, T_1^*}, \varepsilon]$ . These *IMs* are sensitive to occurrence of nonlinearity in isolation system which is mainly reflected in *MBD*. As a result, separation of pulse-like ground motions based on the pulse-period can improve the efficiency for particulate *IMs*. In general, it can be observed that all these *IMs* except for  $[PGA, M]$  have a good efficiency. This can be attributed to the fact that they cover a range of periods and therefore they have a better possibility of capturing the predominant period of the structural response.

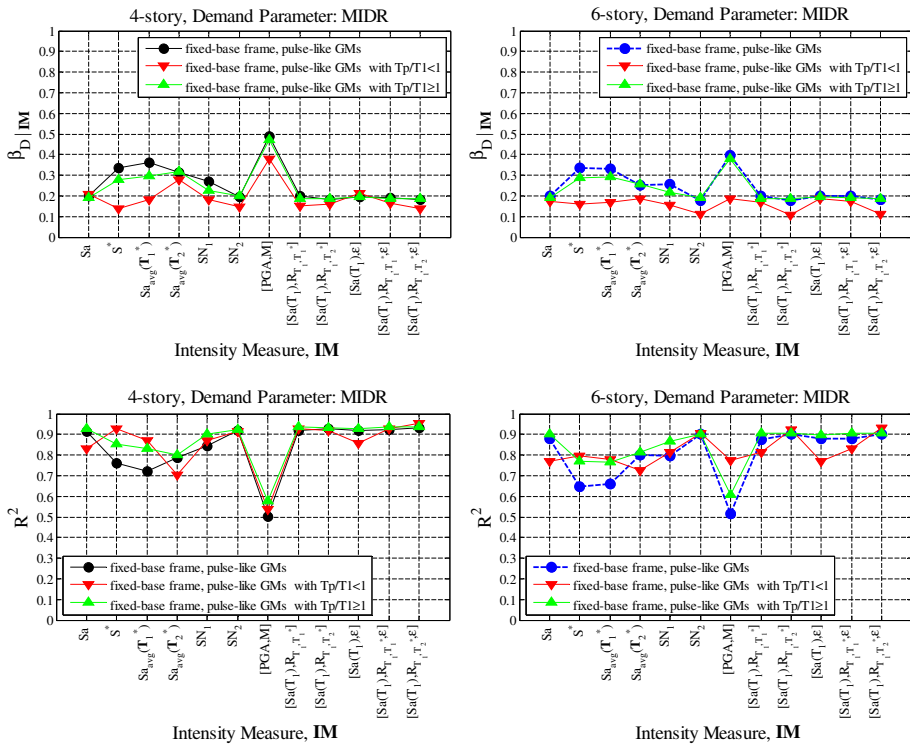


**Fig. 7** Logarithmic standard deviation of regression residuals,  $\beta_{D|IM}$ , and the  $R$ -squared,  $R^2$ , obtained from the cloud analysis of fixed-based structures for the demand parameter *MIDR* and different pulse-like record sets

### 4.4 Results in terms of sufficiency

The RSM in this section is calculated in an approximate manner as explained previously in Sect. 3.2, in Eq. (16) through Eq. (18). Accordingly, the probability model for *DIIM* is calculated based on the lognormal model expressed in Eq. (17).

The reference intensity (i.e.,  $IM_1$  in Eq. 18) is taken to be *Sa* for displacement-based demand parameters (i.e. *MRDR*, *MIDR*, and *MBD*), and *PGA* for acceleration-based demand parameter (i.e. *MFA*); this is mainly due to the fact that these reference intensities not only proved to be efficient, but also are well-known in engineering practice. The sufficiency is measured for each candidate *IM* relative to  $IM_1$ . The relative sufficiency measures are shown in Fig. 9 for both case-study fixed-based buildings and in Fig. 10 for base-isolated buildings equipped with the isolation system  $D_y = 10$  mm. The results reveal that how many extra bits of information, on average, the candidate *IM* gives about the desired structural demand parameter compared to  $IM_1$ . The positive value (above the red dashed line) shows that on average the candidate *IM* provides more information (i.e., is more sufficient) than  $IM_1$ . Similarly, negative values indicates that the candidate *IM* provides on average less information (i.e., is less sufficient) compared to  $IM_1$  for predicting the demand parameter of interest.

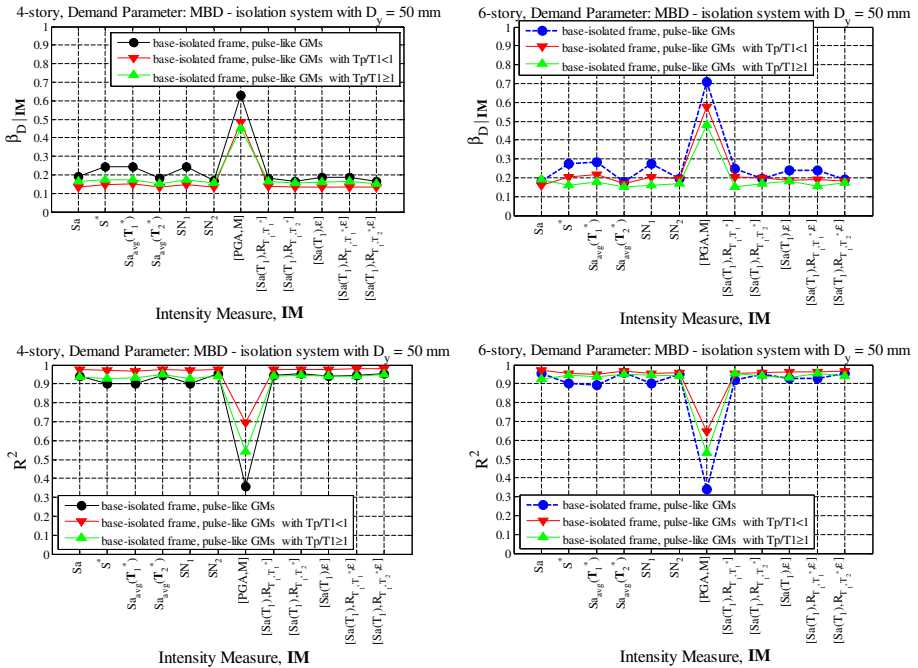


**Fig. 8** Logarithmic standard deviation of regression residuals,  $\beta_{D|IM}$ , and the  $R$ -squared,  $R^2$ , obtained from the cloud analysis of base-isolated structures equipped with isolation system having  $D_y = 50$  mm for demand parameter  $MBD$  and different pulse-like record sets

With reference to Fig. 9, the first eight  $IM$ s having highest RSM's with respect to the reference  $IM_1$  are summarized in Table 9 for various demand parameters associated with the fixed-base structures. Selected  $IM$ s are followed by their RSM's in terms of bits of information ( $>0$ ). It is noteworthy that each outlined RSM in Table 9 is selected based on the maximum estimated values from 4-story and 6-story frames.

Comparing Table 9 (i.e., most relatively sufficient  $IM$ s) with Table 4 (corresponding to the most efficient  $IM$ s) for the fixed-base structures reveals perfect harmony between associated results. Generally, for selecting the proper  $IM$ s for fixed-based buildings based on both efficiency and sufficiency criteria, it is concluded that:

- For displacement-based demand parameters,  $Sa$  is a proper  $IM$  for the case-study fixed-based buildings subjected to ordinary ground motions. For pulse-like ground motion record set, both vector-valued intensities  $[Sa(T_1), R_{T_1, T_2}^*]$  and  $[Sa(T_1), R_{T_1, T_2}^*, \epsilon]$  and to a lower degree the multi-parameter intensity  $S_{N2}$  are the most appropriate  $IM$ s.
- For  $MFA$ ,  $PGA$  is a proper choice. However, for ordinary ground motions, the vector-valued intensities  $[Sa(T_1), R_{T_1, T_2}^*]$  and  $[Sa(T_1), R_{T_1, T_2}^*, \epsilon]$ , the modified integral intensities  $MASI$ ,  $MAVI$ , and  $MI_H$ , and finally the multi-parameter intensities  $S_{N2}$  and  $Sa_{avg}(T_2^*)$  are recommended (see Table 1 for definition of these  $IM$ s). The vector  $[PGA, M]$  is the choice for pulse-like ground motions.

Consistently, the first eight  $IM$ s having the highest RSM's are summarized in Tables 10, 11, 12 and 13 for the base-isolated structures with different isolation properties. Comparing



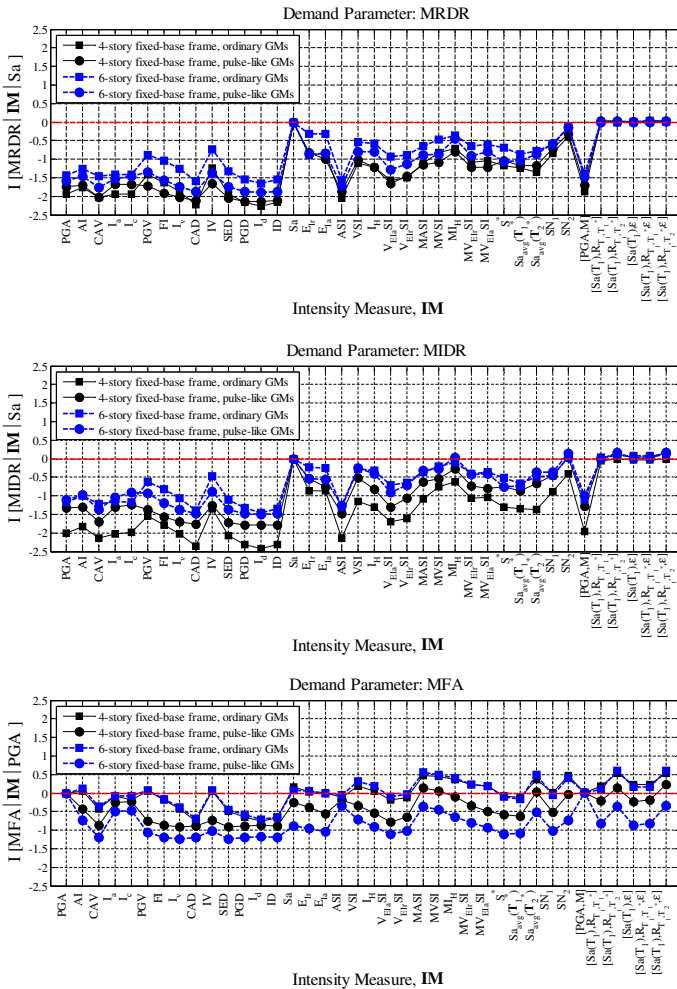


**Fig. 9** The RSM for alternative IMs corresponding to the demand parameters MRDR, MIDR and MFA, for fixed-base buildings subjected to ordinary and pulse-like ground motions

Tables 5, 6, 7 and 8 with Tables 10, 11, 12 and 13 (corresponding to the most efficient IMs) reveals again very good agreement between efficient and sufficient IMs, respectively. Accordingly, the following conclusions can be drawn regarding the proper IMs for base-isolated structures:

- For demand parameters MRDR and MIDR, the most suitable IMs (i.e., are simultaneously sufficient and efficient) for all types of ground-motions are actually the integral scalar intensities comprising MASI, MVSI,  $V_{Ela}SI$  (see Table 1 for their definitions). Accordingly, for ordinary ground motions, it is suggested to use the integral scalar intensities  $V_{Ela}SI$ , and  $I_H$ , while for pulse-like ground motions, the modified integral intensities  $MV_{Ela}SI$ ,  $MI_H$ , and the vector-valued intensity  $[Sa(T_1), R_{T_1, T_2}^*, \varepsilon]$  pass the sufficiency and efficiency requirements. It is to note that other

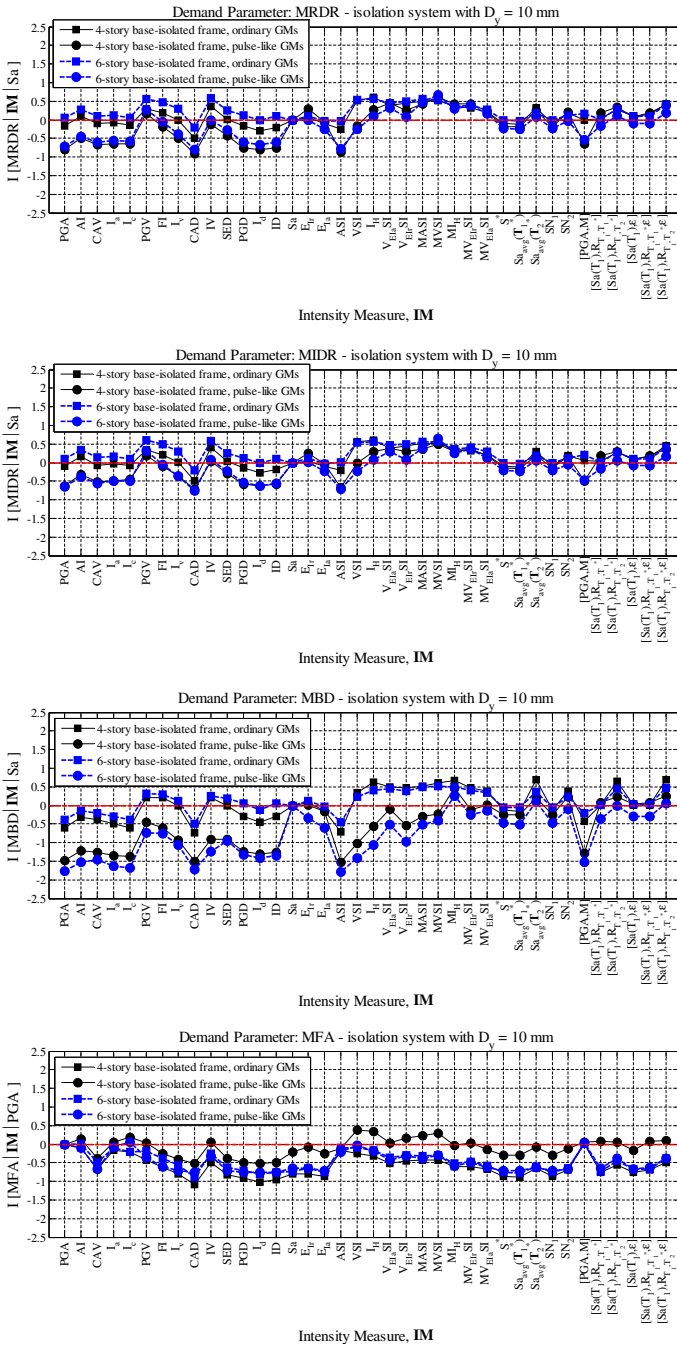


**Fig. 10** The RSM for alternative IMs corresponding to the demand parameters MRDR, MIDR, MBD, and MFA, for base-isolated buildings with isolation system having  $D_y = 10$  mm subjected to ordinary and pulse-like ground motions

**Table 9** The most relatively sufficient *IMs* for fixed-base case-study buildings (with respect to  $\mathbf{IM}_1$ )

$MRDR - \mathbf{IM}_1 = Sa$		$MIDR - \mathbf{IM}_1 = Sa$		$MFA - \mathbf{IM}_1 = PGA$	
Ordinary	Pulse-like	Ordinary	Pulse-like	Ordinary	Pulse-like
$[Sa(T_1), R_{T_1, T_1^*}, \epsilon]$	$[Sa(T_1), R_{T_1, T_2^*}]$	0.030	$[Sa(T_1), R_{T_1, T_2^*}, \epsilon]$	0.164	$[Sa(T_1), R_{T_1, T_2^*}, \epsilon]$
$[Sa(T_1), R_{T_1, T_1^*}]$	$[Sa(T_1), R_{T_1, T_2^*}, \epsilon]$	0.029	$[Sa(T_1), R_{T_1, T_2^*}]$	0.156	$[Sa(T_1), R_{T_1, T_2^*}]$
$[Sa(T_1), R_{T_1, T_2^*}, \epsilon]$		0.015	$S_{N2}$	0.151	<i>MA SI</i>
			$[Sa(T_1), R_{T_1, T_1^*}, \epsilon]$	0.064	<i>MV SI</i>
			$[Sa(T_1), \epsilon]$	0.024	$Sa_{avg}(\mathbf{T}_2^*)$
					$S_{N2}$
					<i>MI<sub>H</sub></i>
					<i>V SI</i>
					0.613
					0.609
					0.556
					0.495
					0.493
					0.467
					0.398
					0.328
					<i>[PGA, M]</i>
					0.0001

**Table 10** The most relatively sufficient *IMs* for base-isolated case-study buildings with  $D_y = 0$  mm (with respect to  $\mathbf{IM}_1$ )

$MRDR - \mathbf{IM}_1 = Sa$		$MIDR - \mathbf{IM}_1 = Sa$		$MBD - \mathbf{IM}_1 = Sa$		$MFA - \mathbf{IM}_1 = PGA$	
Ordinary	Pulse-like	Ordinary	Pulse-like	Ordinary	Pulse-like	Ordinary	Pulse-like
<i>MASI</i>	0.411 <i>MVSI</i>	0.549 <i>VSI</i>	0.463 <i>MVSI</i>	0.670 <i>MVSI</i>	0.705 <i>MI<sub>H</sub></i>	0.561 <i>AI</i>	0.087 <i>I<sub>a</sub></i>
<i>IV</i>	0.391 <i>MI<sub>H</sub></i>	0.452 <i>I<sub>H</sub></i>	0.461 <i>V<sub>ElrSI</sub></i>	0.457 <i>MASI</i>	0.644 <i>S<sub>avg</sub>(T<sub>2</sub><sup>*</sup>)</i>	0.290 <i>I<sub>c</sub></i>	0.083 <i>AI</i>
<i>MVSI</i>	0.385 <i>MV<sub>ElrSI</sub></i>	0.434 <i>MASI</i>	0.459 <i>MV<sub>ElrSI</sub></i>	0.427 [ <i>S<sub>a</sub></i> (T <sub>1</sub> ), <i>R<sub>T<sub>1</sub>,T<sub>2</sub></sub></i> , $\epsilon$ ]	0.612 [ <i>S<sub>a</sub></i> (T <sub>1</sub> ), <i>R<sub>T<sub>1</sub>,T<sub>2</sub></sub></i> , $\epsilon$ ]	0.278 [ <i>PGA</i> , <i>M</i> ]	0.001 [ <i>PGA</i> , <i>M</i> ]
<i>I<sub>H</sub></i>	0.377 <i>V<sub>ElrSI</sub></i>	0.431 <i>MVSI</i>	0.456 <i>MASI</i>	0.372 <i>I<sub>H</sub></i>	0.611 [ <i>S<sub>a</sub></i> (T <sub>1</sub> ), <i>R<sub>T<sub>1</sub>,T<sub>2</sub></sub></i> , $\epsilon$ ]	0.262 <i>I<sub>c</sub></i>	0.022 <i>I<sub>c</sub></i>
<i>PGV</i>	0.369 <i>MASI</i>	0.382 <i>IV</i>	0.454 <i>MI<sub>H</sub></i>	0.358 <i>MI<sub>H</sub></i>	0.607		
<i>VSI</i>	0.363 [ <i>S<sub>a</sub></i> (T <sub>1</sub> ), <i>R<sub>T<sub>1</sub>,T<sub>2</sub></sub></i> , $\epsilon$ ]	0.282 <i>PGV</i>	0.443 <i>PGV</i>	0.346 <i>IV</i>	0.597		
<i>V<sub>ElrSI</sub></i>	0.351 <i>PGV</i>	0.276 <i>V<sub>ElrSI</sub></i>	0.432 [ <i>S<sub>a</sub></i> (T <sub>1</sub> ), <i>R<sub>T<sub>1</sub>,T<sub>2</sub></sub></i> , $\epsilon$ ]	0.313 [ <i>S<sub>a</sub></i> (T <sub>1</sub> ), <i>R<sub>T<sub>1</sub>,T<sub>2</sub></sub></i> , $\epsilon$ ]	0.580		
<i>V<sub>ElrSI</sub></i>	0.337 <i>MV<sub>ElrSI</sub></i>	0.268 <i>V<sub>ElrSI</sub></i>	0.400 <i>V<sub>ElrSI</sub></i>	0.297 <i>PGV</i>	0.578		

**Table 11** The most relatively sufficient *IMs* for base-isolated case-study buildings with  $D_y = 10$  mm (with respect to  $IM_1$ )

$MRDR - IM_1 = Sa$		$MIDR - IM_1 = Sa$		$MBD - IM_1 = Sa$		$MFA - IM_1 = PGA$		
Ordinary	Pulse-like	Ordinary	Pulse-like	Ordinary	Pulse-like	Ordinary	Pulse-like	
$I_H$	0.593 MVSI	0.675 $I_H$	0.604 MVSI	0.650 [ $Sa(T_1), R_{T_1, T_2}^*, \epsilon$ ]	0.690 $MI_H$	0.469 [ $PGA, M$ ]	0.004 $I_c$	0.190
$IV$	0.578 MASI	0.477 PGV	0.602 $V_{EIoSI}$	0.392 $Sa_{avg}(T_2^*)$	0.681 $Sa_{avg}(T_2^*)$	0.254 [ $PGA, M$ ]		0.064
$MASI$	0.564 $V_{EIoSI}$	0.444 $IV$	0.580 MASI	0.379 $MI_H$	0.660 [ $Sa(T_1), R_{T_1, T_2}^*, \epsilon$ ]	0.215		
$PGV$	0.561 $MI_H$	0.437 MASI	0.567 [ $Sa(T_1), R_{T_1, T_2}^*, \epsilon$ ]	0.364 [ $Sa(T_1), R_{T_1, T_2}^*, \epsilon$ ]	0.651			
$MVSI$	0.542 $MV_{EIoSI}$	0.421 MVSI	0.561 $MV_{EIoSI}$	0.363 $I_H$	0.624			
$VSI$	0.533 [ $Sa(T_1), R_{T_1, T_2}^*, \epsilon$ ]	0.415 $VSI$	0.552 PGV	0.317 MVSI	0.598			
$V_{EIoSI}$	0.484 [ $Sa(T_1), R_{T_1, T_2}^*, \epsilon$ ]	0.332 $V_{EIoS}$	0.502 $MI_H$	0.300 MASI	0.525			
$FI$	0.476 PGV	0.284 $FI$	0.501 $I_H$	0.299 $V_{EIoSI}$	0.500			

**Table 12** The most relatively sufficient *IMs* for base-isolated case-study buildings with  $D_y = 25$  mm (with respect to  $IM_1$ )

$MRDR - IM_1 = Sa$		$MIDR - IM_1 = Sa$		$MBD - IM_1 = Sa$		$MFA - IM_1 = PGA$	
Ordinary	Pulse-like	Ordinary	Pulse-like	Ordinary	Pulse-like	Ordinary	Pulse-like
$I_H$	0.674 <i>MVSI</i>	0.662 $I_H$	0.659 <i>MVSI</i>	0.557 $Sa_{avg}(T_2^*)$	0.625 $M I_H$	0.353 $[PGA, M]$	0.031 $I_H$
<i>MVSI</i>	0.634 $[Sa(T_1), R_{T_1, T_2^*}, \epsilon]$	0.481 <i>MVSI</i>	0.626 $[Sa(T_1), R_{T_1, T_2^*}, \epsilon]$	0.367 $M I_H$	0.432 $[Sa(T_1), R_{T_1, T_2^*}, \epsilon]$	0.233	<i>VSI</i>
<i>VSI</i>	0.580 $V_{Ela}SI$	0.466 <i>PGV</i>	0.570 $V_{Ela}SI$	0.347 $[Sa(T_1), R_{T_1, T_2^*}, \epsilon]$	0.431 $Sa_{avg}(T_2^*)$	0.172	<i>MVSI</i>
<i>MASI</i>	0.574 <i>MASI</i>	0.423 <i>VSI</i>	0.561 $[Sa(T_1), R_{T_1, T_2^*}]$	0.312 $[Sa(T_1), R_{T_1, T_2^*}]$	0.406		<i>AI</i>
<i>PGV</i>	0.570 $MV_{Ela}SI$	0.414 <i>MASI</i>	0.558 $MV_{Ela}SI$	0.305 <i>MVSI</i>	0.362		$I_c$
$V_{Ela}SI$	0.558 $[Sa(T_1), R_{T_1, T_2^*}]$	0.398 $V_{Ela}SI$	0.551 <i>MASI</i>	0.297 $V_{Ela}SI$	0.333		$[PGA, M]$
$V_{Ela}SI$	0.490 $M I_H$	0.374 $V_{Ela}SI$	0.484 $M I_H$	0.240 $MV_{Ela}SI$	0.315		$I_a$
<i>IV</i>	0.487 $V_{Ela}SI$	0.322 $[Sa(T_1), R_{T_1, T_2^*}, \epsilon]$	0.483 $Sa_{avg}(T_2^*)$	0.197 $MV_{Ela}SI$	0.282		

**Table 13** The most relatively sufficient *IMs* for base-isolated case-study buildings with  $D_y = 50$  mm (with respect to  $\mathbf{IM}_1$ )

$MRDR - \mathbf{IM}_1 = Sa$		$MIDR - \mathbf{IM}_1 = Sa$		$MBD - \mathbf{IM}_1 = Sa$		$MFA - \mathbf{IM}_1 = PGA$		
Ordinary	Pulse-like	Ordinary	Pulse-like	Ordinary	Pulse-like	Ordinary	Pulse-like	
<i>MVSI</i>	0.580 <i>MVSI</i>	0.487 <i>MVSI</i>	0.531 [ <i>Sa</i> ( $T_1$ ), $R_{T_1, T_2^*}, \epsilon$ ]	0.353 $Sa_{avg}(T_2^*)$	0.560 $Sa_{avg}(T_2^*)$	0.062 [ <i>PGA</i> , <i>M</i> ]	0.072 <i>MVSI</i>	0.771
<i>MASI</i>	0.519 [ <i>Sa</i> ( $T_1$ ), $R_{T_1, T_2^*}, \epsilon$ ]	0.484 $V_{EIPSI}$	0.474 <i>MVSI</i>	0.345 [ <i>Sa</i> ( $T_1$ ), $R_{T_1, T_2^*}, \epsilon$ ]	0.308	<i>AI</i>	0.047 $I_H$	0.740
$V_{EIPSI}$	0.501 $V_{EIPSI}$	0.430 $Sa_{avg}(T_2^*)$	0.466 $V_{EIPSI}$	0.310 $MI_H$	0.278		<i>VSI</i>	0.664
$I_H$	0.498 $MI_H$	0.403 <i>MASI</i>	0.461 [ <i>Sa</i> ( $T_1$ ), $R_{T_1, T_2^*}$ ]	0.300 [ <i>Sa</i> ( $T_1$ ), $R_{T_1, T_2^*}$ ]	0.266		<i>MASI</i>	0.609
$V_{EIPSI}$	0.480 [ <i>Sa</i> ( $T_1$ ), $R_{T_1, T_2^*}$ ]	0.395 $MI_H$	0.457 $MV_{EIPSI}$	0.273 $S_{N2}$	0.226		$V_{EIPSI}$	0.496
$Sa_{avg}(T_2^*)$	0.476 $MV_{EIPSI}$	0.380 $I_H$	0.455 $MI_H$	0.272 [ <i>Sa</i> ( $T_1$ ), $R_{T_1, T_2^*}, \epsilon$ ]	0.070		<i>IV</i>	0.262
$MV_{EIPSI}$	0.465 <i>MASI</i>	0.348 $MV_{EIPSI}$	0.451 <i>MASI</i>	0.231 [ <i>Sa</i> ( $T_1$ ), $\epsilon$ ]	0.043		<i>AI</i>	0.251
$MI_H$	0.457 $Sa_{avg}(T_2^*)$	0.293 $V_{EIPSI}$	0.438 $Sa_{avg}(T_2^*)$	0.199 [ <i>Sa</i> ( $T_1$ ), $R_{T_1, T_2^*}$ ]	0.039		<i>PGV</i>	0.248

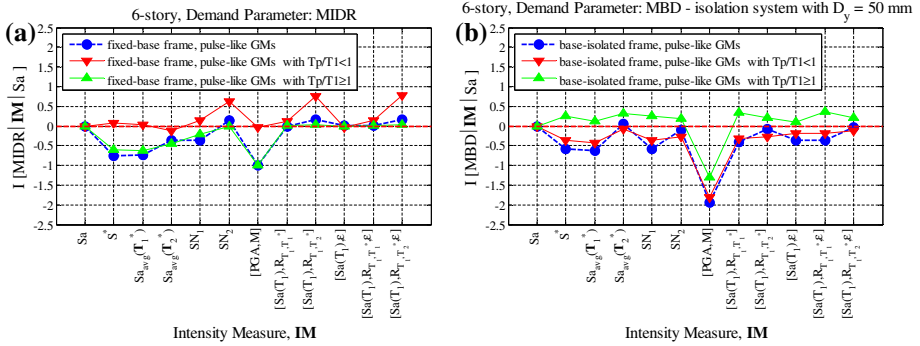


**Fig. 11** Comparison of RSM of alternative *IMs* based on different pulse-like record sets corresponding to **a** *MIDR* associated with the fixed-based 6-story structure, **b** *MBD* associated with the base-isolated 6-story structure

candidate *IMs* are more appropriate for a specific type of isolation system, while the aforementioned ones are applicable to all types of isolation properties.

- For demand parameter *MBD*, suitable *IMs* for all types of ground motions are the modified Housner intensity  $MI_H$ , the multi-parameter intensity  $Sa_{avg}(T_1^*)$ , and vector-valued intensity  $[Sa(T_1), R_{T_1, T_2}, \epsilon]$  and to a lower degree  $[Sa(T_1), R_{T_1, T_2}]$ .
- For the acceleration-based demand *MFA*, proper *IMs* for all types of ground motions are *PGA*,  $[PGA, M]$  and to a lower degree the acceleration-related intensities  $AI$ , and  $I_c$ .

In order to find out the effect of separating pulse-like ground-motion records on the relative sufficiency measure (it has been already investigated for the efficiency results in Sect. 4.3), this measure is plotted in Fig. 11a for *Sa*, multi-parameter, and vector-valued *IMs* corresponding to the demand parameters *MIDR* associated with the 6-story fixed-based structure (see also Fig. 7 for comparison with the efficiency results). Accordingly, for pulse-like records with  $T_p/T_1 < 1$ , the higher-mode sensitive *IMs* including  $SN_2$ ,  $[Sa(T_1), R_{T_1, T_2}]$ , and  $[Sa(T_1), R_{T_1, T_2}, \epsilon]$  have higher sufficiency relative to *Sa*. Moreover, Fig. 11b illustrates the same approach applied to the 6-story base-isolated structures with  $D_y = 50$  mm considering the demand parameter *MBD*. Although no particular improvement in efficiency was previously observed in Fig. 8 for this case, the relative sufficiency, however, reveals an increase for pulse-like records with  $T_p/T_1 > 1$  with respect to  $S^*$ ,  $Sa_{avg}(T_1^*)$ ,  $SN_1$ ,  $[Sa(T_1), R_{T_1, T_1}]$ , and  $[Sa(T_1), R_{T_1, T_1}, \epsilon]$ .<sup>3</sup> It is noteworthy that, with respect to the results reported in terms of efficiency in Fig. 8, separating the pulse-like records based on the pulse period leads to a more significant increase of relative sufficiency in the interested *IMs*.

### 5 Summary and conclusions

The relative capability of a wide range of intensity measures (*IMs*) in predicting the structural response of fixed-based and base-isolated buildings are investigated in terms of efficiency and sufficiency. Cloud analysis, a non-linear dynamic analysis procedure based

<sup>3</sup> As explained previously, these *IMs* are sensitive to occurrence of nonlinearity in isolation system which is mainly reflected in *MBD*.



on linear logarithmic regression of a response parameter versus the adopted *IM*, is employed herein in order to construct a probability model for the demand parameter conditional on the adopted *IM*. The estimated logarithmic standard deviation of the residuals serves as a quantitative measure for predicting the efficiency. The relative sufficiency of alternative *IMs* is calculated by measuring the approximate Relative Sufficiency Measure (RSM) derived earlier by Jalayer et al. (2012). The RSM quantifies the amount of information gained (on average) about a designated structural response parameter by adopting one *IM* instead of another.

The case-study buildings are two typical 4-story and 6-story existing RC moment-resisting frames which are designed according to a previous Italian code. Four alternative peak-related demand parameters, comprising of the maximum roof drift ratio (*MRDR*), maximum inter-story drift ratio (*MIDR*), maximum floor acceleration (*MFA*), and maximum bearing displacement (*MBD*, specifically for base-isolated buildings), together with 38 candidate *IMs* composed of 32 scalar and 6 vector-valued *IMs*, are considered herein. The investigations are made for both ordinary and pulse-like near-fault ground motion records.

In terms of both efficiency and sufficiency assessments, the most suitable *IMs* for predicting alternative demand parameters of fixed-based structures are summarized in Table 14 as follows. Furthermore, the most appropriate *IMs* for predicting alternative demand parameters of base-isolated buildings equipped with different isolation systems are listed in Table 15.

With reference to Tables 14 and 15, it can be concluded that:

- The vector  $[Sa(T_1), R_{T_1, T_2}, \varepsilon]$  and to a lower degree  $[Sa(T_1), R_{T_1, T_2}]$  are capable of predicting displacement-based demand parameters of buildings with different types of base fixity subjected to ordinary and pulse-like ground motions.
- The vector  $[PGA, M]$  is the nominated *IM* for predicting the *MFA* in fixed-base as well as base-isolated buildings.
- The modified Housner *IM*, i.e.  $MI_H$ , is a proper choice for alternative displacement-based demand parameters in base-isolated buildings.
- The most proper *IMs* for predicting the displacement-based demand parameters associated with pulse-like ground motions are generally those that are capable of considering a wide range of periods, i.e. vector-valued or modified *IMs*. This is mainly due to the fact that those *IMs* can better cover the range of pulse periods. Moreover, for acceleration-based demand parameter, *MFA*, the vector  $[PGA, M]$  seems to be the best choice for pulse-like ground motions since it can simultaneously account for the magnitude intensity and the *PGA*.

Furthermore, it is worth noting that the efficiency and especially the relative sufficiency of multi-parameter and vector-valued *IMs* (see Fig. 1) associated with pulse-like ground motions might be affected by the pulse period (or more specifically  $T_p/T_1$  ratio). Hence, in predicting demand parameters associated with pulse-like ground motions, separating the pulse-like records based on the pulse period leads to a more suitable choice of *IMs* in terms of relative sufficiency and efficiency.

It should be finally highlighted that since a large set of ground motions (ordinary and pulse-like) are selected, the efficiency-related findings are presumably not very sensitive to the choice of the ground-motion for the specific structures studied. However, the resulting relative sufficiency values are conditioned on the choice of the probability model for describing the demand parameter given the candidate *IM*. Moreover, this work employs an

**Table 14** The most suitable *IMs* for case-study fixed-based structures

<i>MRDR, MIDR</i>		<i>MFA</i>	
Ordinary	Pulse-like	Ordinary	Pulse-like
$Sa(T_1)^a$	$[Sa(T_1), R_{T_1, T_2^*}, \varepsilon]$	$[Sa(T_1), R_{T_1, T_2^*}, \varepsilon]$	$[PGA, M]$
	$[Sa(T_1), R_{T_1, T_2^*}]$	$[Sa(T_1), R_{T_1, T_2^*}]$	$PGA$
	$S_{N2}$	<i>MASI</i>	
		<i>MVSI</i>	
		$MI_H$	
		<i>PGA</i>	

See Sect. 2 and Table 1 for definition of *IMs*

<sup>a</sup>  $T_1$  is the first-mode period

**Table 15** The most appropriate *IMs* for case-study base-isolated structures

<i>MRDR, MIDR</i>		<i>MBD</i>		<i>MFA</i>	
Ordinary	Pulse-like	Ordinary	Pulse-like	Ordinary	Pulse-like
<i>MVSI</i>	<i>MVSI</i>	$MI_H$	$MI_H$	$[PGA, M]$	$[PGA, M]$
<i>MASI</i>	<i>MASI</i>	$Sa_{avg}(\mathbf{T}_2^*)$	$Sa_{avg}(\mathbf{T}_2^*)$	<i>AI</i>	<i>AI</i>
$V_{El\alpha SI}$	$V_{El\alpha SI}$	$[Sa(T_1), R_{T_1, T_2^*}, \varepsilon]$	$[Sa(T_1), R_{T_1, T_2^*}, \varepsilon]$	$I_c$	$I_c$
$V_{Elr SI}$	$MV_{Elr SI}$	$[Sa(T_1), R_{T_1, T_2^*}]$	$[Sa(T_1), R_{T_1, T_2^*}]$		
$I_H$	$MI_H$				
	$[Sa(T_1), R_{T_1, T_2^*}, \varepsilon]$				

See Sect. 2 and Table 1 for definition of *IMs*

approximate RSM (from Eq. 18) as a simple screening tool for raking various candidate scalar and vector-valued *IMs*. The approximate expression presented in Eq. (18) is based on the assumption that various plausible ground motions are equally likely to take place. However, it should be emphasized that RSM is calculated more rigorously by resolving the integral in Eq. (15) by simulation. In this case, one needs to adopt an appropriate stochastic ground motion model in order to be able to simulate ground motions from a probability distribution (see Jalayer et al. 2012 for a comprehensive example). As a result, the ranking of *IMs* presented in this work in terms of their relative sufficiency should be regarded as a preliminary one. A more refined ranking can be established once suitable stochastic ground motion models for ordinary and near-source conditions are adopted.

As a final word for future developments, the investigations should also be carried out by implementing energy-based demand parameters and intensity measures. Elaborations on this study can lead towards identifying a pool of most suitable *IMs* for probabilistic seismic demand assessment for alternative classes of existing RC buildings (of course taking into account also their predictability through probabilistic seismic hazard analysis).

**Acknowledgments** This work was supported in part by DPC-Reluis 2014–2016 and National Operative Program Project METROPOLIS 2014-16. This support is gratefully acknowledged. Any opinions, findings, and conclusions or recommendations expressed in this material are those of the authors and do not necessarily reflect those of the sponsor.

## References

- Akkar S, Özen Ö (2005) Effect of peak ground velocity on deformation demands for SDOF systems. *Earthq Eng Struct Dyn* 34(13):1551–1571
- Avşar Ö, Özdenmir G (2013) Response of seismic-isolated bridges in relation to intensity measures of ordinary and pulse-like ground motions. *J Bridge Eng* 18(3):250–260
- Baker JW (2007) Quantitative classification of near-fault ground motions using wavelet analysis. *Bull Seismol Soc Am* 97(5):1486–1501
- Baker JW, Cornell CA (2006) Spectral shape, epsilon and record selection. *Earthq Eng Struct Dyn* 35(9):1077–1095
- Baker JW, Cornell CA (2008a) Vector-valued intensity measures incorporating spectral shape for prediction of structural response. *J Earthq Eng* 12(4):534–554
- Baker JW, Cornell CA (2008b) Vector-valued intensity measures for pulse-like near-fault ground motions. *Eng Struct* 30(4):1048–1057
- Benavent-Climent A, Pujades LG, López-Almansa F (2002) Design energy input spectra for moderate-seismicity regions. *Earthq Eng Struct Dyn* 31(5):1151–1172
- Bianchini M, Diotallevi P, Baker JW (2009) Prediction of inelastic structural response using an average of spectral accelerations. In: Proceedings of 10th international conference on structural safety and reliability (ICOSSAR09), Osaka, Japan
- Campbell KW, Bozorgnia Y (2008) NGA ground motion model for the geometric mean horizontal component of PGA, PGV, PGD and 5% damped linear elastic response spectra for periods ranging from 0.01 to 10s. *Earthq Spectra* 24(1):139–171
- Chiou B, Darragh R, Gregor N, Silva W (2008) NGA project strong-motion database. *Earthq Spectra* 24(1):23–44
- Cordova PP, Deierlein GG, Mehanny SS, Cornell CA (2000) Development of a two-parameter seismic intensity measure and probabilistic assessment procedure. In: Proceedings of the 2nd US-Japan workshop on Performance-Based Earthquake Engineering Methodology for reinforced concrete building structures, Sapporo, Hokkaido, pp 187–206
- Cornell CA, Krawinkler H (2000) Progress and challenges in seismic performance assessment. *PEER Cent News* 3(2)
- Decreto Ministero (DM) dei Lavori Pubblici 16/01/1996 (1996) Norme Tecniche per le Costruzioni in Zone Sismiche (in Italian). Italian Ministry of Public Works, Rome, Italy
- Ebrahimian H, Jalayer F, Lucchini A, Mollaioli F, de Dominicis R (2014) Case studies on relative sufficiency of alternative intensity measures of ground shaking. In: Second European conference on earthquake engineering and seismology (2ECEES), Istanbul, Turkey, Aug 24–29
- Elefante L, Jalayer F, Iervolino I, Manfredi G (2010) Disaggregation-based response weighting scheme for seismic risk assessment of structures. *Soil Dyn Earthq Eng* 30(2):1513–1527
- Giovenale P, Cornell CA, Esteva L (2004) Comparing the adequacy of alternative ground motion intensity measures for the estimation of structural responses. *Earthq Eng Struct Dyn* 33(8):951–979
- Jalayer F, Beck JL (2008) Effect of the alternative representations of ground motion uncertainty on seismic risk assessment of structures. *Earthq Eng Struct Dyn* 37(1):61–79
- Jalayer F, Cornell CA (2003) A technical framework for probability-based demand and capacity factor design (DCFD) seismic formats. Pacific Earthquake Engineering Center (PEER), 2003/2008
- Jalayer F, Cornell CA (2009) Alternative non-linear demand estimation methods for probability-based seismic assessments. *Earthq Eng Struct Dyn* 38(8):951–972
- Jalayer F, Beck J, Zareian F (2012) Analyzing the sufficiency of alternative scalar and vector intensity measures of ground shaking based on information theory. *J Eng Mech* 138(3):307–316
- Jalayer F, De Risi R, Manfredi G (2015) Bayesian cloud analysis: efficient structural fragility assessment using linear regression. *Bull Earthq Eng* 13:1183–1203
- Jayaram N, Mollaioli F, Bazzurro P, De Sortis A, Bruno S (2010) Prediction of structural response of reinforced concrete frames subjected to earthquake ground motions. In: Proceedings of 9th US National and 10th Canadian conference on earthquake engineering, Toronto, Canada, 25–29 July, pp 428–437
- Kalkan E, Kunnath SK (2007) Effective cyclic energy as a measure of seismic demand. *J Earthq Eng* 11(5):725–751
- Kullback S, Leibler RA (1951) On information and sufficiency. *Ann Math Stat* 22(1):79–86
- Lin L, Naumoski N, Saatcioglu N, Foo S (2011) Improved intensity measures for probabilistic seismic demand analysis. Part 1: development of improved intensity measures. *Can J Civ Eng* 38(1):79–88

- López-Almansa F, Yazgan AU, Benavent-Climent A (2013) Design energy input spectra for high seismicity regions based on Turkish registers. *Bull Earthq Eng* 11(4):885–912
- Lucchini A, Mollaioli F, Monti G (2011) Intensity measures for response prediction of a torsional building subjected to bi-directional earthquake ground motion. *Bull Earthq Eng* 9(5):1499–1518
- Luco N, Cornell CA (2007) Structure-specific scalar intensity measures for near-source and ordinary earthquake ground motions. *Earthq Spectra* 23(2):357–392
- Luco N, Manuel L, Baldava S, Bazzurro P (2005) Correlation of damage of steel moment-resisting frames to a vector-valued set of ground motion parameter. In: *Proceedings of the 9th international conference on structural safety and reliability (ICOSSAR05)*, Rome, Italy, pp 2719–2726
- Moehle JP, Deierlein GG (2004) A framework methodology for performance-based earthquake engineering. In: *Proceedings of the 13th world conference on earthquake engineering*, Vancouver, Canada, 1–6 August
- Mollaioli F, Bruno S, Decanini L, Saragoni R (2011) Correlations between energy and displacement demands for performance-based seismic engineering. *Pure appl Geophys* 168(1–2):237–259
- Mollaioli F, Lucchini A, Cheng Y, Monti G (2013) Intensity measures for the seismic response prediction of base-isolated buildings. *Bull Earthq Eng* 11(5):1841–1866
- Mori Y, Yamanaka T, Luco N, Nakashima M, Cornell CA (2004) Predictors of seismic demand of SMRF buildings considering post-elastic mode shape. In: *Proceedings of 13th world conference on earthquake engineering*, Vancouver, Canada, 1–6 August
- Nurtuğ A, Sucuoğlu H (1995) Prediction of seismic energy dissipation in SDOF systems. *Earthq Eng Struct Dyn* 24(9):1215–1223
- OpenSees (2010) Open system for earthquake engineering simulation, version 2.2.2, Pacific earthquake engineering research center, <http://opensees.berkeley.edu>
- Pacific Earthquake Engineering Research (PEER) (2005) Next generation attenuation (NGA) project. <http://peer.berkeley.edu/nga/>
- Riddell R (2007) On ground motion intensity indice. *Earthq Spectra* 23(1):147–173
- Shahi SK (2013) A probabilistic framework to include the effects of near-fault directivity in seismic hazard assessment. Dissertation, Stanford University
- Shahi SK, Baker JW (2011) An empirically calibrated framework for including the effects of near-fault directivity in probabilistic seismic hazard analysis. *Bull Seismol Soc Am* 101(2):742–755
- Shome N, Cornell CA (1999) Probabilistic seismic demand analysis of nonlinear structures. RMS Program, Stanford University, Report No. RMS35. <https://blume.stanford.edu/rms-reports>. Accessed 2 June 2014
- Shome N, Cornell CA, Bazzurro P, Carballo JE (1998) Earthquakes, records, and nonlinear responses. *Earthq Spectra* 14(3):469–500
- Sucuoğlu H, Erberik A (2004) Energy-based hysteresis and damage models for deteriorating systems. *Earthq Eng Struct Dyn* 33(1):69–88
- Vamvatsikos D, Cornell CA (2005) Developing efficient scalar and vector intensity measures for IDA capacity estimation by incorporating elastic spectral shape information. *Earthq Eng Struct Dyn* 34(13):1573–1600
- Yakut A, Yilmaz H (2008) Correlation of deformation demands with ground motion intensity. *J Struct Eng* 134(12):1818–1828